

RECORD
2022/2

GEOLOGY AND MINERALIZATION POTENTIAL OF THE GERRY WELL GREENSTONE BELT (COLLURABBIE REGION), NORTHEASTERN YILGARN CRATON

LL Grech, Y Lu, Y Wang, Y Gao, B Qian, M You and TJ Beardsmore



Government of Western Australia
Department of Mines, Industry Regulation
and Safety

Geological Survey of
Western Australia





Government of **Western Australia**
Department of **Mines, Industry Regulation
and Safety**

RECORD 2022/2

GEOLOGY AND MINERALIZATION POTENTIAL OF THE GERRY WELL GREENSTONE BELT (COLLURABBIE REGION), NORTHEASTERN YILGARN CRATON

by

LL Grech, Y Lu, Y Wang*, Y Gao*, B Qian*, M You* and TJ Beardsmore

* Xi'an Center, China Geological Survey, 438 East Youyi Rd, Beilin District, Xi'an, Shaanxi Province, China

PERTH 2022



**Geological Survey of
Western Australia**

MINISTER FOR MINES AND PETROLEUM
Hon Bill Johnston MLA

DIRECTOR GENERAL, DEPARTMENT OF MINES, INDUSTRY REGULATION AND SAFETY
Richard Sellers

EXECUTIVE DIRECTOR, GEOLOGICAL SURVEY AND RESOURCE STRATEGY
Jeff Haworth

REFERENCE

The recommended reference for this publication is:

Grech, LL, Lu, Y, Wang, Y, Gao, Y, Qian, B, You, M and Beardsmore, TJ 2022, Geology and mineralization potential of the Gerry Well greenstone belt (Collurabie region), northeastern Yilgarn Craton: Geological Survey of Western Australia, Record 2022/2, 19p.

ISBN 978-1-74168-924-2

ISSN 2204-4345

Grid references in this publication refer to the Geocentric Datum of Australia 1994 (GDA94). Locations mentioned in the text are referenced using Map Grid Australia (MGA) coordinates, Zone 51. All locations are quoted to at least the nearest 100 m.



Disclaimer

This product uses information from various sources. The Department of Mines, Industry Regulation and Safety (DMIRS) and the State cannot guarantee the accuracy, currency or completeness of the information. Neither the department nor the State of Western Australia nor any employee or agent of the department shall be responsible or liable for any loss, damage or injury arising from the use of or reliance on any information, data or advice (including incomplete, out of date, incorrect, inaccurate or misleading information, data or advice) expressed or implied in, or coming from, this publication or incorporated into it by reference, by any person whatsoever.

Published 2022 by the Geological Survey of Western Australia

This Record is published in digital format (PDF) and is available online at <www.dmirs.wa.gov.au/GSWApublications>.



© State of Western Australia (Department of Mines, Industry Regulation and Safety) 2022

With the exception of the Western Australian Coat of Arms and other logos, and where otherwise noted, these data are provided under a Creative Commons Attribution 4.0 International Licence. (<http://creativecommons.org/licenses/by/4.0/legalcode>)

Further details of geoscience products are available from:

First floor counter
Department of Mines, Industry Regulation and Safety
100 Plain Street
EAST PERTH WESTERN AUSTRALIA 6004
Telephone: +61 8 9222 3459 Email: publications@dmirs.wa.gov.au
www.dmirs.wa.gov.au/GSWApublications

Cover image: Journey to the centre of the Kimberley (© 2010 PL Schubert)

Contents

Abstract	1
Introduction	1
Regional geological setting	1
Sampling and analytical techniques	4
Geochronology	4
Geochemistry	4
Hyperspectral data	4
Results	6
Local lithological distribution	6
Mineralogy	6
Hyperspectral characteristics of the Collurabbie drillcores	6
Whole-rock geochemistry	6
Ultramafic rocks	6
Basaltic rocks	8
Sanukitoid rocks	8
Geochronology	10
Discussion	10
Geochemistry and mineralogy of ultramafic rocks	10
Significance of felsic magmatic events in the Collurabbie region	15
Mineralization potential of the Gerry Well greenstone belt	15
Nickel mineralization	15
Gold mineralization	16
Conclusion	17
Acknowledgements	17
References	17

Appendices

All appendices are available with the PDF online as an accompanying digital resource

1. Whole-rock geochemical data: major elements recalculated for volatile content
2. Portable X-ray fluorescence (pXRF) data: raw, uncorrected
3. Lithological, hyperspectral, and whole-rock geochemical downhole plots

Figures

1. Generalized geological map of the Eastern Goldfields Superterrane	2
2. Drillcore logs (crosscutting dolerite dykes excluded)	7
3. Possible peperite in drillhole CXDD002	8
4. Examples of preserved primary volcanic textures in the Gerry Well greenstone belt komatiites	8
5. Example of a sanukitoid-like unit	9
6. Deformed ultramafic rock in a drillhole	9
7. Ni/Ti vs Ni/Cr ratios discriminating komatiitic rock types	9
8. A Ni vs Cr plot discerning the different fields within a komatiitic system	10
9. Incompatible trace element ratios of Zr/TiO ₂ , La/Sm, Th/Nb, and Th/Yb in ultramafic samples	11
10. Rare earth element (REE) patterns of komatiitic rocks of the Gerry Well greenstone belt	12
11. Al ₂ O ₃ /TiO ₂ ratios for ultramafic rock samples from the Gerry Well greenstone belt	12
12. TiO ₂ /Th, TiO ₂ /Zr, TiO ₂ /Nb, and TiO ₂ /La ratios for basalts from the Gerry Well greenstone belt	13
13. Comparison of chemistry between the sanukitoid-like units collected in this study, and other sanukitoids in the Eastern Goldfields Superterrane	14
14. Cathodoluminescence image of representative zircons from sample 235282	14
15. U–Pb analytical data for zircons from sample 235282	15

Tables

1. Geochronological and lithological characteristics of the terranes comprising the Yilgarn Craton	3
2. Collar information for the studied drillcore	5

Geology and mineralization potential of the Gerry Well greenstone belt (Collurabbie region), northeastern Yilgarn Craton

LL Grech, Y Lu, Y Wang*, Y Gao*, B Qian*, M You* and TJ Beardsmore

Abstract

The Gerry Well greenstone belt (Collurabbie region) in the Burtville Terrane, northeastern Yilgarn Craton, is a current focus of exploration for komatiite-hosted nickel sulfides and orogenic gold mineralization. Knowledge of the lithostratigraphy, age, geochemical characteristics of this area, and hence, its prospectivity for nickel and gold mineral systems, has been improved with geological logging and hyperspectral, geochemical and geochronological analysis of samples from eight diamond drillcores. The geochemistry and mineralogical characteristics of the komatiites suggest that their prospectivity for major nickel sulfide mineralization is comparatively low, although recent discoveries of Ni–Cu–Co–PGE (platinum group elements) sulfide mineralization indicate that further work is required to understand the metallogenic potential of the region. Dating of a sanukitoid-like unit that is interpreted to be younger than the komatiites has yielded a magmatic crystallization age of 2713 ± 3 Ma. This is older than the previously documented (2.68 – 2.66 Ga) sanukitoid events in the Eastern Goldfields Superterrane (EGST) and confirms that komatiites in the Gerry Well greenstone belt are older than the c. 2.7 Ga komatiites of the Kalgoorlie Terrane. Sanukitoids elsewhere in the Yilgarn Craton have an apparent spatial and temporal association with gold mineralization. Their presence in the Gerry Well greenstone belt may indicate prospectivity for significant gold in this region, related to an event older than that currently recognized in the EGST.

KEYWORDS: Archean, Burtville Terrane, gold, komatiite, nickel, sanukitoid, Yilgarn Craton

Introduction

The Kalgoorlie Terrane of the Eastern Goldfields Superterrane (EGST) in Western Australia hosts many types of mineral deposits, including komatiite-hosted nickel, orogenic gold, volcanogenic massive sulfides, and banded iron-formations. Mineral exploration in the EGST has predominantly focused on the Kalgoorlie Terrane, leaving the eastern terranes less explored and less understood. This report describes new studies of the Gerry Well greenstone belt in the Collurabbie region within the Burtville Terrane in the northeastern Yilgarn Craton (Fig. 1). Historical exploration for komatiite-hosted nickel sulfides in this area has made no economic discoveries, but companies undertaking more recent work are optimistic that the region contains such deposits and has the potential to also host gold mineralization (e.g. Rox Resources Limited, 2021).

This contribution presents new mineralogical, geochemical, and geochronological data from the Gerry Well greenstone belt that inform our understanding of its overall geology and mineralization potential.

Regional geological setting

The Gerry Well greenstone belt lies in the Collurabbie region, in the northeastern Burtville Terrane. It is extensively covered by Cenozoic material, and its stratigraphy and

age are therefore poorly constrained, though it is known to comprise Archean sedimentary, mafic, ultramafic, felsic volcanic, and volcanoclastic rocks that are metamorphosed mostly to greenschist facies, and locally amphibolite facies along the margins of the belt (Champion and Stewart, 1996; Jones, 2006; Dykmans, 2008). The greenstone belt is in fault contact with Archean granitic rocks along the northern extensions of the intensely sheared Lulu and De La Poer Faults (Dykmans, 2008).

The Burtville Terrane is one of four fault-bounded terranes making up the EGST, in the eastern half of the Yilgarn Craton (Swager et al., 1992; Swager, 1997; Cassidy et al., 2006; Czarnota et al., 2008; Fig. 1). A summary of the Yilgarn Craton terrane ages and lithologies, including those comprising the EGST, is presented in Table 1.

Many of the greenstone belts in the EGST contain ultramafic rocks, including komatiites. The majority of komatiites occur in the Kalgoorlie Terrane, and have ages between c. 2.71 and 2.68 Ga (Nelson, 1997). However, there are older komatiites known in the Kurnalpi and Burtville Terranes, including the 2.8 Ga komatiite sequence at Mt Windarra (Barley et al., 2006), and 2.94 – 2.84 Ga komatiites in the Mt Fisher greenstone belt (Mole et al., 2016). Numerous world-class nickel deposits are hosted by the 2.7 Ga komatiites of the Kalgoorlie Terrane (e.g. Mt Keith and Perseverance deposits in the Agnew–Wiluna greenstone belt), but recent discoveries of nickel sulfide mineralization in the older komatiites in the Burtville Terrane (e.g. Rosie, Fisher East, Dragon, Cambridge; Fig. 1) suggest that the geographic and stratigraphic search spaces for such deposits could be significantly expanded.

* Xi'an Center, China Geological Survey, 438 East Youyi Rd, Beilin District, Xi'an, Shaanxi Province, China

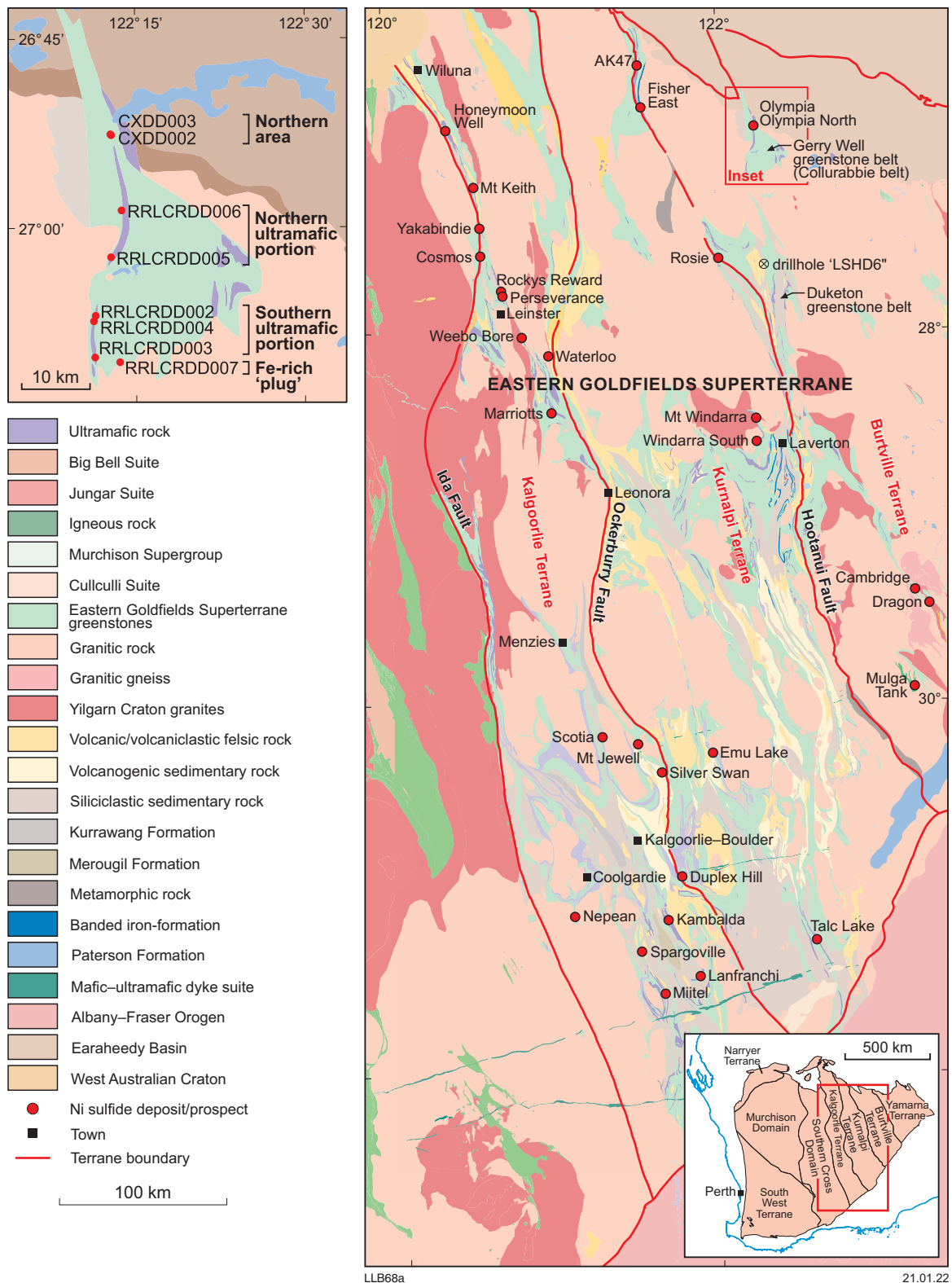


Figure 1. Generalized geological map of the Eastern Goldfields Superterrane, with selected nickel deposits and prospects shown after Burley and Barnes (2019). Terrane boundaries from Martin et al. (2016a). Insert top left: Gerry Well greenstone belt showing the locations of the studied drillcores. Geology and structural lines from Martin et al. (2016b)

Table 1. Geochronological and lithological characteristics of the terranes comprising the Yilgarn Craton, from Witt et al., 2020

<i>Terrane</i>	<i>Age of greenstone deposition (Ma)</i>	<i>Lithology</i>	<i>Age of granite emplacement (Ma)</i>	<i>Xenocryst and detrital zircon ages (Ma)</i>	<i>Reference</i>
Southwest	3200–2850 2715–2675	Metasedimentary (Jimperding, Chittering, Balingup) Mafic to felsic volcanics (Saddleback)	3240–2920, 2880–2820, 2805–2720, 2720–2600	Metasedimentary: 3855–2940 Granites: 2650–3150	Allibone et al., 1998; Mole et al., 2012, 2013; Stein et al., 2001; Thern and Nelson, 2012; Wilde and Pidgeon, 1986; Wilde et al., 1996
Narryer	3730–<3065	Meta-anorthosite, mafic–ultramafic volcanics, metasedimentary (Jack Hills, Mt Narryer)	Gneisses: 3680–2995 Granites: 3730–2600	Metasedimentary: 4400–3065	Kinny et al., 1988; Mole et al., 2013; Rasmussen et al., 2011; Thern and Nelson, 2012
Youanmi (Murchison)	2960–2935 2825–2800 2800–2700	Felsic volcanics (Goldern Grove Group, Wongan Hills) Mafic and felsic volcanics (Norie Group) and mafic layered intrusions Mafic to felsic volcanics (Polelle Group) and metasedimentary + mafic to felsic volcanics (Glen Group)	2810–2600	3670–2730	Cassidy et al., 2002; Ivanic et al., 2010, 2012; Mole et al., 2012; Pidgeon and Wilde, 1990; Van Kranendonk and Ivanic, 2009
Youanmi (Southern Cross)	<3130 >2900 2735–2720 <2675	Metasedimentary (Illaara, Maynard Hills, Gum Creek) Felsic volcanic (Ravensthorpe), felsic volcanic (Johnson Lakes) Intermediate to felsic volcanics (Marda, Gum Creek) Metasedimentary sequence, Southern Cross greenstone belt	3155–2617	Metasedimentary: 4350–3130 Granites: 2820–2620	Cassidy et al., 2002; Chen et al., 2003; Mole et al., 2012; Morris and Kirkland, 2014; Romano et al., 2010; Thebaud and Miller, 2009; Witt, 1998; Wyche et al., 2004
Kalgoorlie	2950–2920 2730–>2750 2720–2690 2690–2660 <2665	Mafic and felsic volcanics, metasedimentary (Norseman) Mafic (Leonora, Kathleen Valley?, Agnew) Mafic–ultramafic volcanics (Kambalda Group) Intermediate to felsic volcanics (Kalgoorlie Group) Late-stage sedimentary basins	2700–2640 (High-Ca granites) 2660–2630 (Low-Ca granites) 2720–2640 (Mafic granites)	Granites and felsic volcanic rocks: 2710–2670, 2760–2720, 2810–2790, 2910–2880, 2970–2950	Baggot, 2006; Campbell and Hill, 1988; Cassidy et al., 2002; Czarnota et al., 2010; Krapez and Pickard, 2010; Mole et al., 2013; Squire et al., 2010; Swager, 1997; Witt et al., 2001
Kurnalpi and Gindalbie	<2870 2810–2755 2720–2700 2705–2675 2690–2680 <2665	Mafic volcanics, banded iron-formation (Dingo Range) Mafic and metasedimentary (Laverton) Mafic to intermediate volcanics (Minerie, Sunrise Dam, Ida Hill, Bore Well) Felsic volcanic, volcanoclastics Bimodal volcanics (Gindalbie) Late-stage sedimentary basins	2675–2640 (High-Ca granites) 2660–2630 (Low-Ca granites) 2720–2640 (Mafic granites) 2670–2630 (Syenitic granites) 2720–2675 (HFSE-enriched granites)	3200–2700	Barley et al., 2008; Brown et al., 2002; Cassidy et al., 2002; Czarnota et al., 2010; Dunphy et al., 2003; Kositcin et al., 2008; Krapez and Pickard, 2010; Mole et al., 2013; Nelson, 1997; Swager, 1997
Burtville	2960–2800 2775–2715	Mainly mafic volcanics Felsic volcanics, clastic metasedimentary	2930–2645	Greenstones: 2969–2910 Granites: 2930–2695	Pawley et al., 2012
Yamarna	2700–2675	Felsic volcanics (Toppin Hill Formation)	2830–2710	Greenstones: 2730 Granites: 2815–2800	Pawley et al., 2012

Note: HFSE, high field strength elements

The greenstone belts of the Yilgarn Craton are intruded by a variety of felsic magmas. Of these, sanukitoid magmas are considered to have particular metallogenic importance due to their apparent spatial and temporal links with gold mineralization (e.g. Witt et al., 2013; Witt et al., 2015; Smithies et al., 2018). A sanukitoid is defined as a monzodioritic, dioritic to granodioritic intrusive rock, typically containing hornblende (\pm clinopyroxene) with high concentrations of Cr, Ni, large ion lithophile elements, and a high Mg# ($=\text{mol Mg}/[\text{Mg}+\text{Fe}_{\text{tot}}]$, with Fe_{tot} being all Fe calculated as Fe^{2+}) (Smithies et al., 2018). At 60 wt% SiO_2 , sanukitoids generally have a Mg# >60, Ni and Cr concentrations of >100 ppm, and Ba and Sr concentrations of >1000 ppm (Shirey and Hanson, 1984; Stern et al., 1989; Smithies and Champion, 2000; Martin et al., 2005; Smithies et al., 2018). Sanukitoids are included within the 'Mafic granite' group of Champion and Sheraton (1997) and Cassidy et al. (2002), and are thought to have formed either from the melting of the metasomatized mantle along with lamprophyres (Shirey and Hanson, 1984; Rock and Groves, 1988a; Rock and Groves, 1988b; Rock et al., 1989; Stern et al., 1989; Smithies and Champion, 2000; Martin et al., 2005) or by fractionation from lamprophyric magmas (Perring and Rock, 1991; Smithies et al., 2018). In either case, it is widely accepted that sanukitoids and lamprophyres are typically associated with large lithospheric structures (Smithies et al., 2018). Sanukitoid emplacement in the EGST mostly occurred between c. 2.68 and 2.66 Ga (Smithies et al., 2018), although the enriched magmatism leading to such rock types can probably be dated back to 2708 ± 7 Ma (Nelson, 1996; Nelson, 1997).

Sampling and analytical techniques

Eight stratigraphically representative drillcores were selected from four distinct parts of the Gerry Well greenstone belt: the Northern Area (CXDD002-003; Olympia North prospect), the Northern Ultramafic Portion (RRLCRDD005-006), the Southern Ultramafic Portion (RRLCRDD002-004), and an interpreted Fe-rich intrusive 'plug' in the south (RRLCRDD007; Fig. 1; Table 2). The selected drillholes are limited to the western side of the greenstone belt, as there is limited diamond drilling elsewhere. Each drillcore was geologically and hyperspectrally logged and sampled for petrographical, geochemical, and geochronological analysis. Samples for geochemistry were also taken from a dacitic unit and a granodioritic unit from drillcore LSHD6 in the Duketon greenstone belt, where previous geochronological work has been undertaken (Fig. 1; Table 2).

Geochronology

A sample of a tonalitic sanukitoid-like unit (GSWA 235282) that intrudes sulfidic sedimentary rock was collected from drillhole RRLCRDD002 for geochronology (Figs 1, 2). A single homogeneous sample was composited from several short intervals (112.2 – 112.45 m, 112.51 – 112.64 m, 112.8 – 113.23 m, and 113.5 – 113.8 m) that were separated by mafic dykes and enclaves. The sample was analysed using the Sensitive High-Resolution Ion Microprobe (SHRIMP-B) instrument at the John de Laeter Centre at Curtin University. Details of the analytical procedure are provided by Lu et al. (2020).

Geochemistry

One hundred and twenty-eight representative samples of drillcore were selected for whole-rock geochemical analysis. Veins and xenoliths were excluded where possible, and weathered material was removed prior to sample crushing at the Geological Survey of Western Australia (GSWA) Sample Preparation Laboratory at the Perth Core Library, Western Australia. Analyses were determined by Bureau Veritas (Perth, Western Australia) on all but four samples of granodiorite from drillhole LSHD6, which were analysed at ALS Global (Perth, Western Australia). Both laboratories measured major element oxides by X-ray fluorescence (XRF) spectrometry. Bureau Veritas analysed trace elements using Li-borate fusion and laser ablation inductively coupled plasma mass spectrometry, and analysed Au, Pt, and Pd by fire assay and inductively coupled plasma mass spectrometry (ICP-MS). ALS analysed trace elements using Li-borate fusion then acid dilution or mixed acid digest, followed by ICP-MS. This laboratory analysed gold by Aqua Regia and ICP-MS, but did not measure Pt or Pd. Specific analytical techniques are reported in Appendix 1. Reference materials and duplicates were submitted to assure data quality. The major element data reported here have been corrected to exclude volatile content (see Appendix 1). Portable XRF (pXRF) data were also collected for drillcores from the Gerry Well greenstone belt, but are not discussed further in this report. The raw, uncorrected data are provided in Appendix 2.

Hyperspectral data

The mineralogy of the diamond drillcore from the Collurabbie region was acquired using HyLogger-3, and analysed using the methodology described by Hancock and Huntington (2010), Hancock et al. (2013), and Schodlok et al. (2016). Reflectance spectra were collected over the visible-to-near infrared (VNIR 380–1000 nm), shortwave infrared (SWIR 1000–2500 nm), and thermal infrared (TIR 6000–14500 nm) wavelength ranges to determine the presence, abundance, composition, and other characteristics of a range of common rock-forming minerals. High-resolution (0.1 mm pixel) digital colour photographs of the core were obtained concurrently, using a built-in line scan camera. The reflectance spectra were automatically resampled at 8 nm spectral sampling and 8 mm spatial resolution by The Spectral Geologist software (TSG).

Raw (resampled) HyLogger-3 spectral data were initially processed automatically using The Spectral Assistant (TSA) algorithm built into TSG software (Huntington et al., 1997; Schodlok et al., 2016). TSA compared the drillcore spectra against modelled mixtures of 'typical' mineral spectra from a reference library, to identify two (for VNIR and SWIR) or three (for TIR) best-matched minerals, and estimate their relative proportions and fitting errors (Huntington et al., 1997). Extensive QA/QC of individual core trays was undertaken by HyLogger staff to ensure that unwanted sections of the trays were adequately masked and the spectra for these sections were not presented. Interactive depth logging was performed to account for core loss and nominate accurate depth points. Automated mineral identifications were subsequently validated to filter out obviously erroneous interpretations by manually refining the three mineral-matching scalars (uTSAV, uTSAS, and uTSAT) used by TSA, and testing the results against the interpretations obtained using additional

Table 2. Collar information for the studied drillcore

<i>Drillhole</i>	<i>Drilling operator</i>	<i>WAMEX Report ID</i>	<i>Original Datum</i>	<i>Zone</i>	<i>Latitude (degrees)</i>	<i>Longitude (degrees)</i>	<i>Easting</i>	<i>Northing</i>	<i>Map sheet 100K</i>	<i>Map sheet 250K</i>	<i>Elevation (m RL)</i>	<i>Inclination (degrees)</i>	<i>Azimuth (degrees)</i>
CXDD002	Rox Resources	A118432	GDA94	51	-26.8774	122.2145	421979	7026902	Collurabbie 3344	Kingston SG 51-10	514.79	-60	90
CXDD003	Rox Resources	A118432	GDA94	51	-26.8764	122.2137	421897	7027007	Collurabbie 3344	Kingston SG 51-10	515.21	-60	90
RRLCRDD002	Regis Resources	A78701	GDA94	51	-27.1152	122.1916	419887.5	7000559	Urarey 3343	Duketon SG 51-14	536.4	-50	270
RRLCRDD003	Regis Resources	A98257	GDA94	51	-27.1703	122.1906	419822.5	6994460	Urarey 3343	Duketon SG 51-14	518.87	-50	270
RRLCRDD004	Regis Resources	A78701	GDA94	51	-27.1222	122.1889	419627.1	6999784	Urarey 3343	Duketon SG 51-14	544.546	-50	270
RRLCRDD005	Regis Resources	A78701	GDA94	51	-27.0377	122.2149	422137.1	7009160	Urarey 3343	Duketon SG 51-14	531.153	-50	270
RRLCRDD006	Regis Resources	A78701	GDA94	51	-26.976	122.2306	423659	7016012	Collurabbie 3344	Kingston SG 51-10	522.93	-50	90
RRLCRDD007	Regis Resources	A78701	GDA94	51	-27.1782	122.2257	423314.1	6993608	Urarey 3343	Duketon SG 51-14	512	-50	277
LSHD6	Western Mining Corporation	A10686	GDA94	51	-27.6532	122.3149	432426	6941018	Duketon 3342	Duketon SG 51-14	na	-60	270

Note: na, not available

scalars built into TSG (e.g. core albedo and colour), and scalars generated by the multiple feature extraction method of Cudahy et al. (2008). All available digital HyLogger data and interpretation files are available from the manager of the HyLogger facility on request. Associated GSWA Reports, Records, and summary histograms can be downloaded from the Department of Mines, Industry Regulation and Safety (DMIRS) eBookshop and GeoVIEW.WA. Summary logs of the lithology, HyLogger-derived mineralogy, and geochemistry for the eight drillcores used in the study are provided in Appendix 3. The records documenting specific HyLogger data for each drillhole mentioned in this report can be found via the Department of Mines, Industry Regulation and Safety's (DMIRS) online GeoVIEW.WA portal and the DMIRS eBookshop (see Hancock et al., 2020 for access instructions).

Results

Local lithological distribution

The geology of the Collurabbie region is poorly understood because the Archean Gerry Well greenstone belt is extensively covered by Cenozoic material (Champion and Stewart, 1996; Jones, 2006). Lithostratigraphy has been inferred entirely from the magnetic data and selected diamond drillcore obtained for nickel exploration from close to the western margin of the greenstone belt. Stratigraphic relationships are rarely evident in the drillcores, and possibly only locally relevant; more regional stratigraphic and structural studies are required to establish context.

The Northern Area of the Gerry Well greenstone belt (Northern Area) comprises quartz-feldspar porphyritic rocks, ultramafic rocks, basalts, and a mafic intrusion (Fig. 2). The ultramafic units are <15 m thick and completely altered to either talc-carbonate or serpentine, with no preserved primary igneous textures. Peperite-like textures are evident in drillhole CXDD002, suggesting magma emplacement into an older sedimentary unit (Fig. 3). In drillhole CXDD003, the ultramafic contacts with basalt are highly deformed, with abundant veining and brecciation occurring at the up-hole contact. The nature of the ultramafic contacts in this area suggest that these units may be intrusive rather than flows or that they occurred in a flanking environment adjacent to a main flow channel. More evidence is needed to verify either possibility.

Ultramafic rocks are more abundant to the south. Rock types in the Northern Ultramafic Portion include granodiorite, undifferentiated ultramafic rocks, sedimentary rocks, and basalts, which are all intruded by younger dolerites (Fig. 2). Deformation, metamorphism and weathering of the rocks is greatest in this part of the greenstone belt, and they are commonly strongly veined. For example, in diamond drillhole RRLCRDD005, where undifferentiated ultramafic rocks are strongly foliated and locally partially to almost completely overprinted by sporadically folded veining that comprises carbonate, chlorite, quartz and/or serpentine.

The Southern Ultramafic Portion of the greenstone belt contains talc-carbonate- and serpentine-altered ultramafic and komatiitic rocks, basalts, various sedimentary rocks (including sulfidic chert), and a sanukitoid-like intrusion (Fig. 2). Primary igneous textures in the ultramafic rocks are

best preserved in this area (e.g. Fig. 4a–c). The sanukitoid-like rock occurs in drillhole RRLCRDD002, where though altered is recognizably broadly tonalitic, comprising 55% plagioclase (in places replaced by sericite and epidote), 25% quartz, 10% biotite (in places replaced by chlorite), and 5% K-feldspar (Lu et al., 2020). It contains abundant fine-grained mafic and tonalitic-dioritic, locally sulfide-bearing xenoliths throughout, and is crosscut by fine-grained mafic dykes (Fig. 5). The unit is interpreted to have intruded older, sulfidic sedimentary rocks that are broadly contemporaneous with the komatiites. New U–Pb dating of zircon (Lu et al., 2020) from this sanukitoid-like rock is reported in 'Geochronology' below.

There is a strongly magnetic 'plug' at the southern limit of the greenstone belt (intersected in drillhole RRLCRDD007; Fig. 1). This Fe-rich unit contains intervals of peridotite and abundant disseminated sulfides (likely pyrrhotite). An intrusive gabbro lies up-hole of this unit that is in turn overlain by a thin sedimentary rock unit intruded by numerous pegmatites. A granitic intrusive unit is at the top of the hole (Fig. 2).

Most rock units in the drillholes are strongly foliated, more so throughout the Northern Ultramafic Portion of the greenstone (Fig. 6). The tectonic significance of this deformation fabric is unclear.

Mineralogy

Hyperspectral characteristics of the Collurabbie drillcores

The dominant rock types in the drillcores are serpentine-altered ultramafic rocks, talc-carbonate-altered ultramafic rocks, basalts, and a variety of sedimentary rocks. HyLogger-3 data records a distinct mineralogy for each rock type. The serpentine-altered ultramafic rocks are dominated by serpentine ± amphibole ± chlorite ± dark mica ± olivine ± pyroxene ± carbonate. The talc-carbonate-altered ultramafic rocks contain abundant talc and carbonate ± chlorite ± amphiboles. Basalts are distinguished by their abundant chlorite and amphibole content, although they also contain minor amounts of plagioclase and quartz, carbonate, white mica, and sporadic epidote (e.g. drillhole RRLCRDD004, Appendix 3). Sedimentary rocks are typically dominated by chlorite and white mica (evident in SWIR data), and quartz (evident in TIR data), regardless of the specific rock type (e.g. shale, chert).

Whole-rock geochemistry

Ultramafic rocks

The lithogeochemistry of ultramafic/komatiitic rocks can provide information on the origin of the magmas and vectors towards nickel sulfide mineralization. For this study, the least-altered samples were selected for geochemical analysis, although the absence of primary igneous textures, the abundance of hydrous and carbonate minerals, and high loss-on-ignition (LOI) concentrations in all analysed ultramafic rocks indicate that even these rock types have been significantly altered by hydrothermal fluids (Appendix 1).

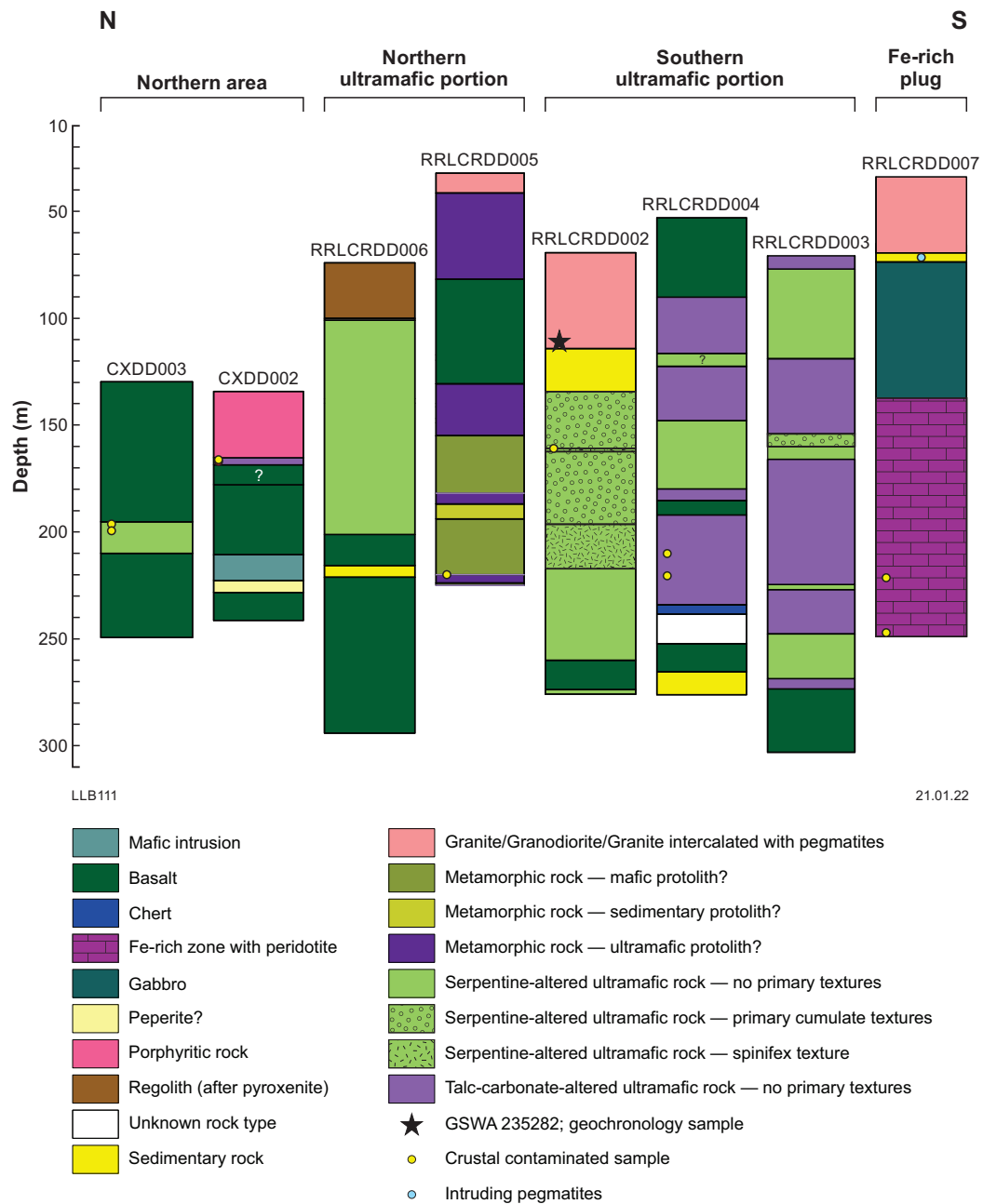


Figure 2. Drillcore logs (with crosscutting dolerite dykes excluded) for drillholes RRLCRDD002–007 and CXDD002–003. The locations of the ultramafic samples showing crustal contamination are denoted in yellow circles. The blue circle on the log for RRLCRDD007 indicates where abundant pegmatites intrude metasedimentary rock

Nevertheless, the observed alteration appears to have occurred largely by the addition of volatile components (water, carbon dioxide) and lithogeochemical data that are normalized to exclude these components believed to closely represent primary magmatic compositions. Some samples of ultramafic rocks (e.g. from RRLCRDD005) are interpreted to be ultramafic on the basis of their geochemistry alone, as the protoliths could not be otherwise discerned. Other samples (e.g. in drillhole RRLCRDD007) are anomalously Fe-rich, probably due to the presence of abundant Fe sulfides.

Samples classified as komatiitic or unassigned ultramafic rocks show a broad range in composition (39.59 – 51.41 wt% SiO₂, 5.19 – 46.19 wt% MgO, 0.18 – 14.74 wt% Al₂O₃, 0.01 – 0.76 wt% TiO₂, 4–5010 ppm Ni, 4–14,000 ppm Cr, and 1.5 – 40 ppm Zr). The data are presented in a variety of geochemical plots that are useful for assessing nickel prospectivity (Figures 7–11), and are discussed below. It is worth noting that one ultramafic sample (GSWA 238340 in drillhole CXDD002) has comparatively high Pt and Pd values (Appendix 1).



Figure 3. Possible peperite in drillhole CXDD002, approximately 221.7 – 227 m

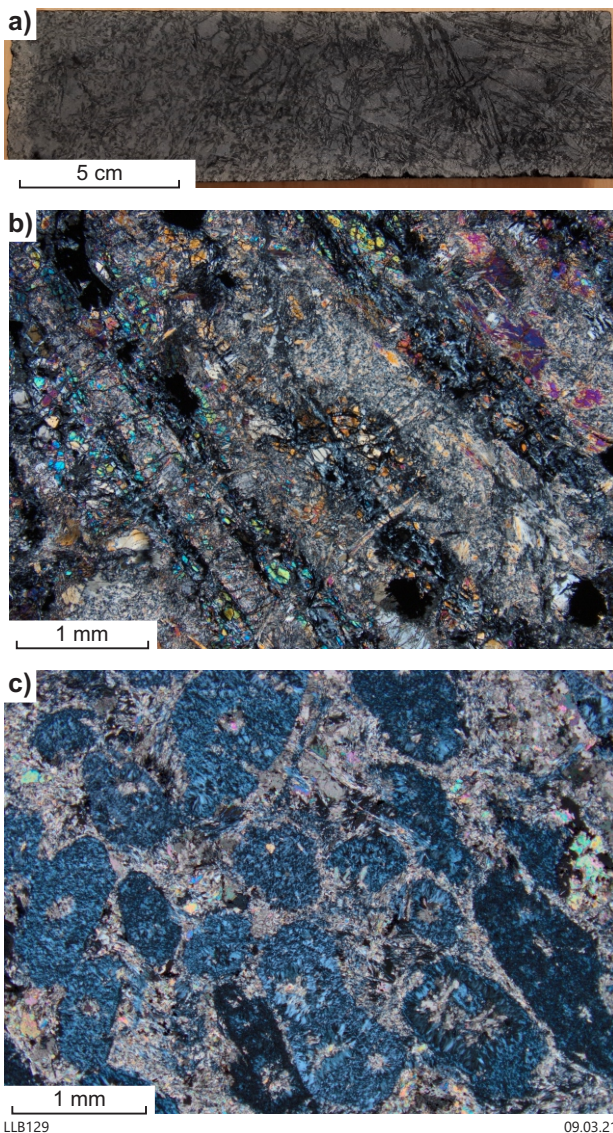


Figure 4. Examples of preserved primary volcanic textures in the Gerry Well greenstone belt komatiites: a) komatiite with preserved spinifex-texture from drillhole RRLCRDD002, 208.9 – 209.08 m; b) plane-polarized, transmitted light photomicrograph of the spinifex-texture in a komatiite from drillhole RRLCRDD002, 206.07 – 206.23 m; c) plane-polarized, transmitted light photomicrograph of the cumulate texture in a komatiite from drillhole RRLCRDD003, 259.85 – 260 m.

Basaltic rocks

The whole-rock lithogeochemistry of the samples of least-altered basaltic rocks from the Gerry Well greenstone belt suggests that most are low-thorium basalts (LTB), with compositions falling in the ranges 48–55 wt% SiO_2 , 14.1 – 15.3 wt% Al_2O_3 , 0.6 – 0.95 wt% TiO_2 , 9.5 – 11 wt% CaO , 0.06 – 0.1 wt% P_2O_5 , and an Mg# between 39 and 62 (after Barnes et al., 2012; Smithies et al., 2017). Samples from the Southern Ultramafic Portion of the greenstone belt (drillholes RRLCRDD002–004) have compositions that closely match these parameters. Samples from the Northern Ultramafic Portion (drillholes RRLCRDD005 and 006) have lower contents of P_2O_5 , TiO_2 , Al_2O_3 , and a higher Mg# overall, but have Th/TiO_2 , Zr/TiO_2 , Nb/TiO_2 , and La/TiO_2 ratios that are consistent with LTBs (Fig. 12). However, basalt samples from the Far Northern Area (drillholes CXDD002 and 003) commonly have particularly high TiO_2 (mostly 1.75 – 3.0 wt%; one outlier at 0.8 wt% TiO_2) and P_2O_5 (0.05 – 0.26 wt%), and on average a lower Mg#. These rocks are not LTBs, although they could be high-Ti tholeiites.

Sanukitoid rocks

The whole-rock lithogeochemistry of the sanukitoid-like unit in drillhole RRLCRDD002 was determined for three least-altered, xenolith-free samples. The average composition is 69 wt% SiO_2 , Mg# 37, 19 ppm Ni, 58 ppm Cr, 283 ppm Sr, and 557 ppm Ba (Fig. 13). Its chemical identification as sanukitoid-like is based on the relatively high concentrations of the trace elements compared with other felsic rock types at a given silica content. However, identification as sanukitoid-like is particularly difficult at ≥ 70 wt% silica content because the trace element abundances are much lower than those of more typical sanukitoids, probably reflecting a high degree of fractionation. Its hydrous mineralogy (biotite clots after hornblende) and presence of abundant mafic enclaves are similar to sanukitoid-like rocks elsewhere in the EGST (e.g. Smithies et al., 2018), but this rock cannot be confirmed as a true sanukitoid without comparison to related, less-fractionated samples from the region.



Figure 5. Example of the sanukitoid-like unit from drillhole RRLCRDD002, 99.8 – 104.2 m

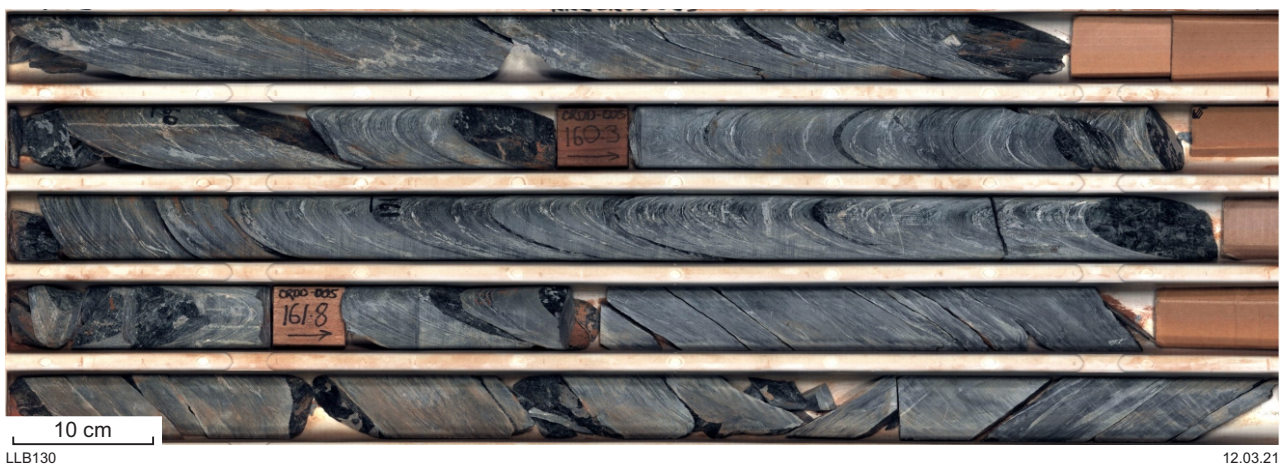


Figure 6. Deformed ultramafic rock from drillhole RRLCRDD005; 159.2 – 163.3 m

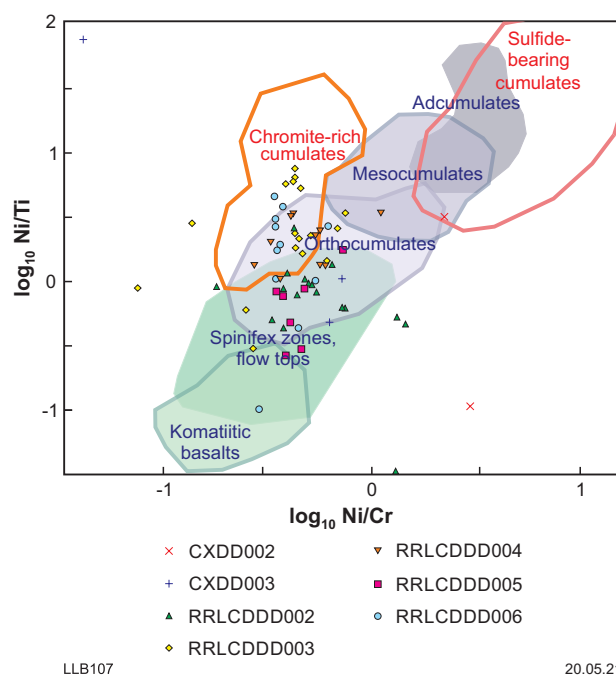


Figure 7. Ni/Ti vs Ni/Cr ratios discriminating komatiitic rock types from RRLCRDD002–007, CXDD002, and 003. Rock-type fields are from Le Vaillant et al. (2016)

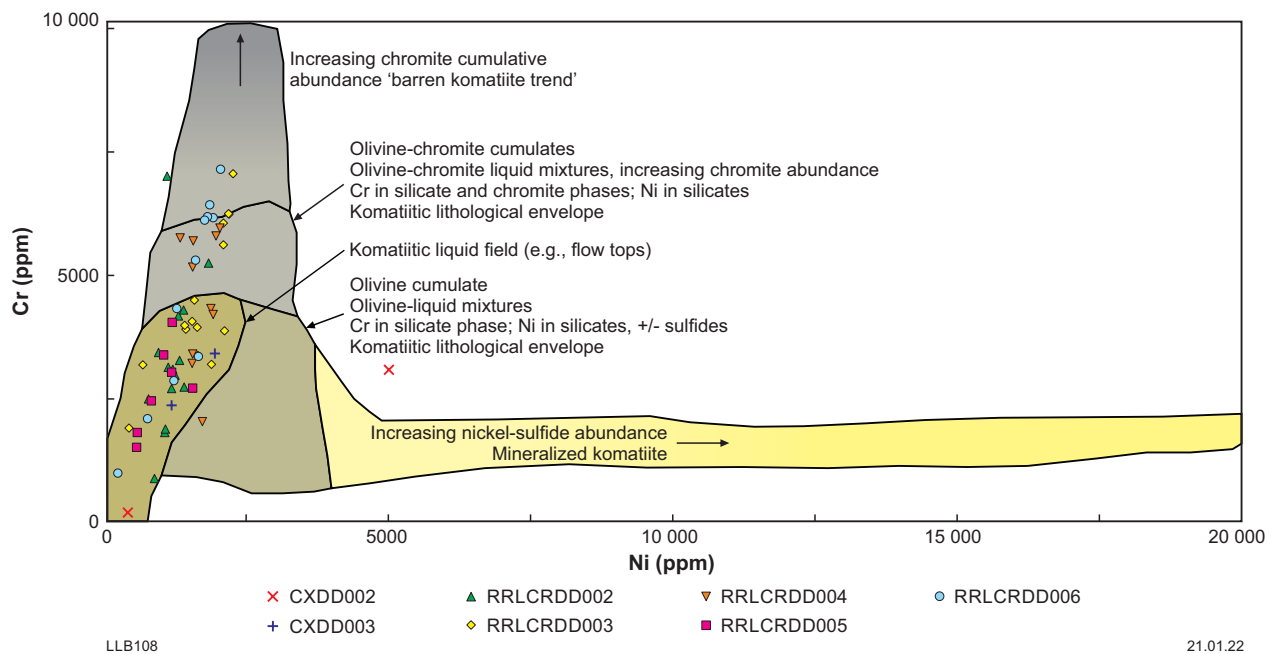


Figure 8. Ni vs Cr plot discerning different textural and mineralogical fields within a komatiitic system. Figure after Brand (1999)

Geochronology

Lu et al. (2020) analysed zircons from the sanukitoid-like rock in drillhole RRLCRDD002 (Sample GSWA 235282). These zircons are colourless to pale brown, and subhedral to euhedral. The crystals are up to 300- μ m long, equant to elongate with aspect ratios up to 4:1, and exhibit ubiquitous concentric zoning in cathodoluminescence images (Fig. 14; Lu et al., 2020).

Twenty-two analyses were obtained from 22 zircons. The results are concordant to strongly discordant (Fig. 15). Three analyses are >5% discordant, and are considered unreliable and not geologically significant (Group D). The remaining 19 analyses can be divided into two groups based on their $^{207}\text{Pb}^*/^{206}\text{Pb}^*$ ratios. Group P (one analysis) yielded a $^{207}\text{Pb}^*/^{206}\text{Pb}^*$ date of 2693 ± 6 Ma (1σ). Group I (18 analyses) yielded a weighted mean of $^{207}\text{Pb}^*/^{206}\text{Pb}^*$ date of 2713 ± 3 Ma (mean square of weighted deviates = 0.80), which is interpreted to be the magmatic crystallization age of the sanukitoid-like unit. The Group P date of 2693 ± 6 Ma (1σ) is inferred to result from an ancient loss of radiogenic Pb (Lu et al., 2020).

Discussion

Geochemistry and mineralogy of ultramafic rocks

All the talc-carbonate- and serpentine-altered ultramafic rocks sampled from drillholes CXDD002 and 003, RRLCRDD002–004, and RRLCRDD006 have high MgO,

Cr, and Ni, and lower SiO_2 , Zr, Al_2O_3 , and TiO_2 abundances compared with other rock types, regardless of the alteration type or intensity (Appendix 3). However, individual ultramafic units that appear to be uniformly altered do show internal variations in their MgO, Cr, and Ni contents, features attributed to original internal mineralogical and textural differentiation in these units (e.g. orthocumulate- vs mesocumulate-textured; best seen in drillhole RRLCRDD004; Appendix 3). HyLogger-3 and geochemical data were used to infer the likely mineral and textural features of the protoliths of the extremely deformed, metamorphosed, and altered samples from drillhole RRLCRDD005, which otherwise show compositional and mineralogical patterns similar (albeit less consistently so) to ultramafic rocks in the other drillholes CXDD002 and 003, and RRLCRDD002–004, 003, 004 and 006 (Appendix 3).

The peridotite-bearing, Fe-rich 'plug' in drillhole RRLCRDD007 is rich in iron sulfides, and there is a change from a carbonate \pm sulfate \pm silica \pm K-feldspar \pm plagioclase \pm pyroxene \pm white mica \pm kaolin assemblage in the up-hole part of the unit to a pyroxene \pm silica \pm carbonate \pm white mica \pm amphibole \pm kaolin \pm K-feldspar \pm plagioclase \pm sulfate \pm olivine \pm epidote (and minor amounts of AlOH and smectite) assemblage in the downhole part. All geochemical data are from samples from the downhole part of the unit, and indicate that it is different to ultramafic rocks in the other drillholes. Its MgO content is <10 wt%, but is about the same as that of the gabbroic unit up-hole (Appendix 3). All elements that are typically low in komatiites (Al_2O_3 , TiO_2 , Zr, and SiO_2) are also low in peridotite, and Ni and Cr are particularly low. The Fe-rich 'plug' could possibly be the peridotitic to pyroxenitic cumulate basal part of the overlying gabbroic unit.

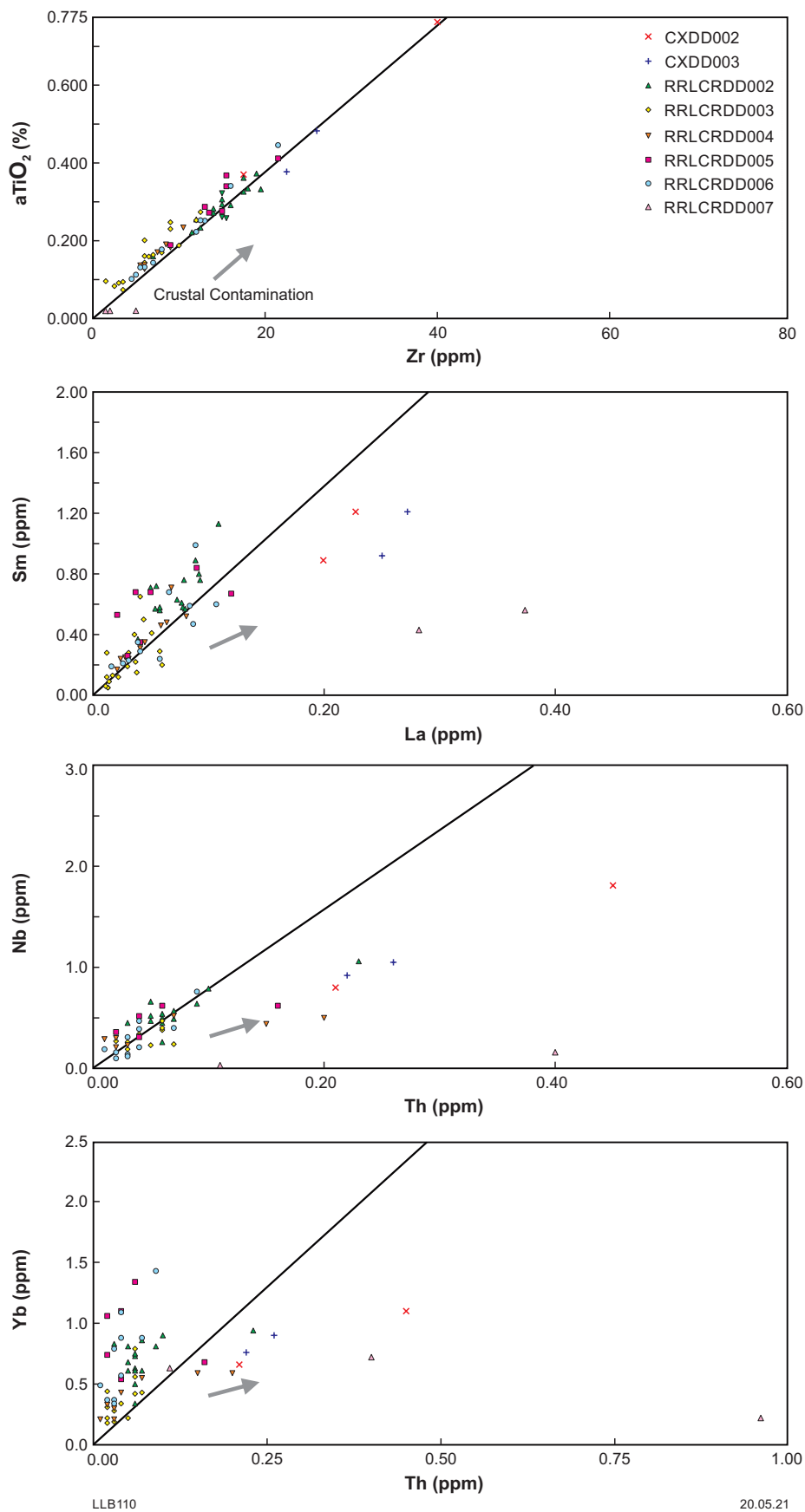


Figure 9. Incompatible trace element ratios for ultramafic samples from drillholes RRLCRDD002–007, CXDD002 and CXDD003: a) Zr/TiO₂, b) La/Sm, c) Th/Nb, and d) Th/Yb. The heavy black line represents the assumed pristine mantle ratio for each element pair after McDonough and Sun (1995). Data trends that deviate from the line in the direction of the arrow represent likely crustal contamination trends

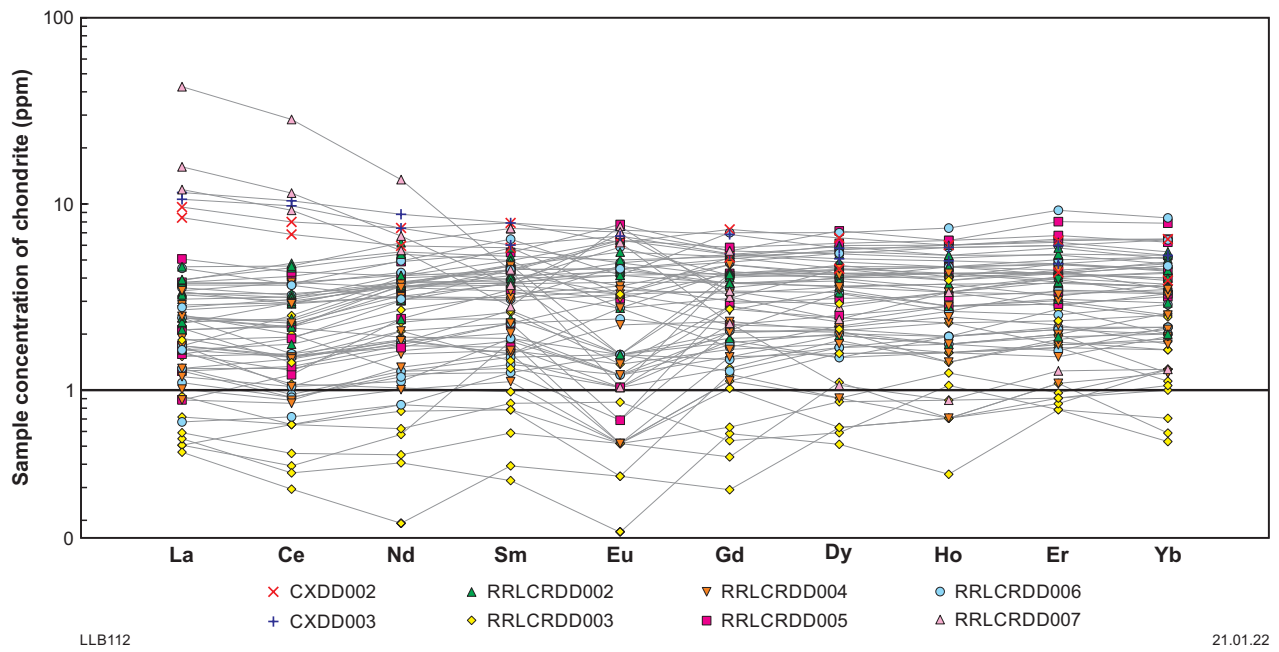


Figure 10. Rare earth element (REE) compositions for komatiitic rocks of the Gerry Well greenstone belt, normalized using C1 chondrite values (following Sun and McDonough, 1989)

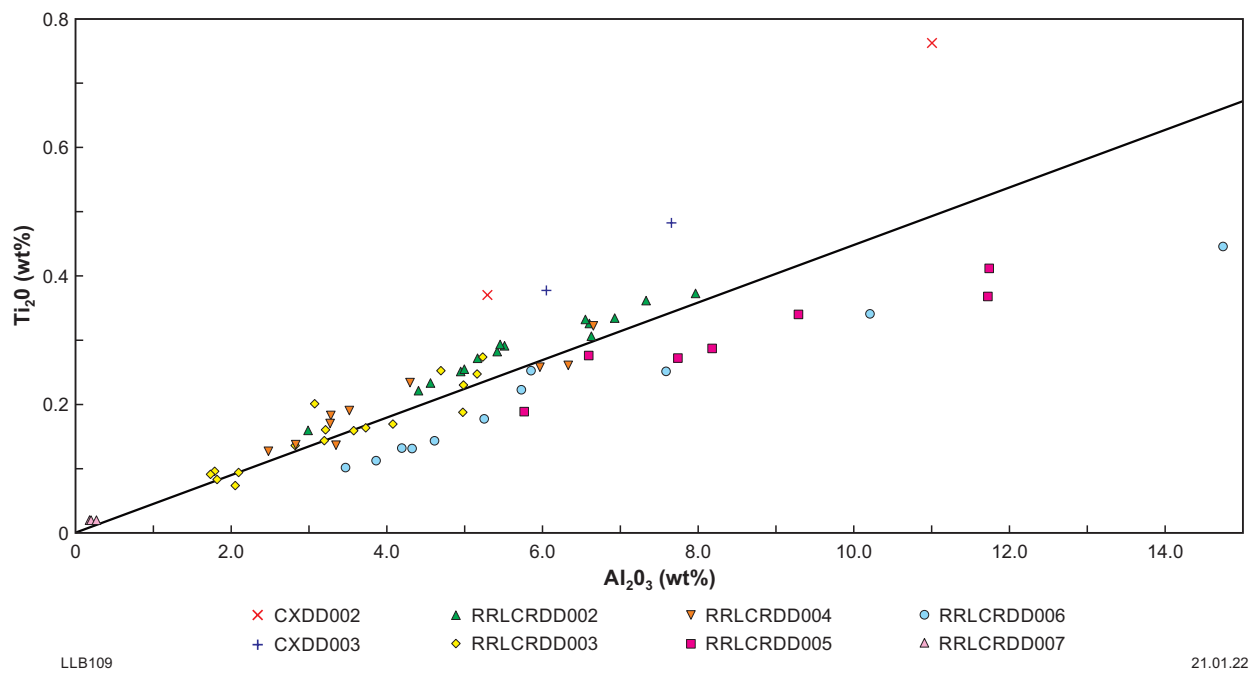


Figure 11. Volatile-free $\text{Al}_2\text{O}_3/\text{TiO}_2$ ratios of the samples from RRLCRDD002–007, CXDD002 and 003. The chondritic mantle line is shown in black, from Barnes (2006)

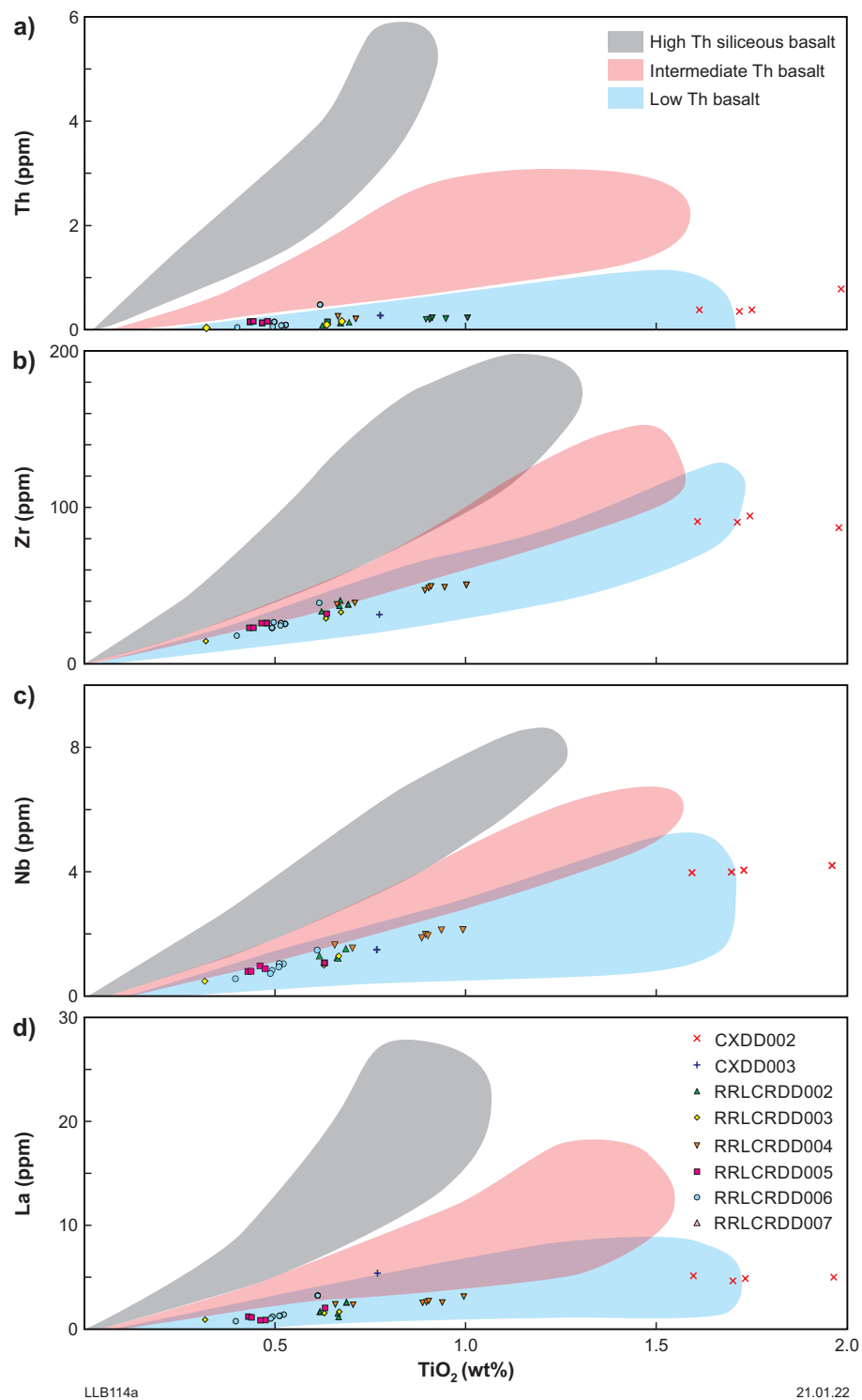


Figure 12. Volatile-free trace element ratios for the majority of basalt samples from the Gerry Well greenstone belt; a) TiO_2/Th , b) TiO_2/Zr , c) TiO_2/Nb , and d) TiO_2/La . Not appearing on these plots are samples from drillholes CXDD002 and CXDD003, that have TiO_2 values exceeding 2 wt%. Basalt-'type' fields are from Barnes et al. (2012)

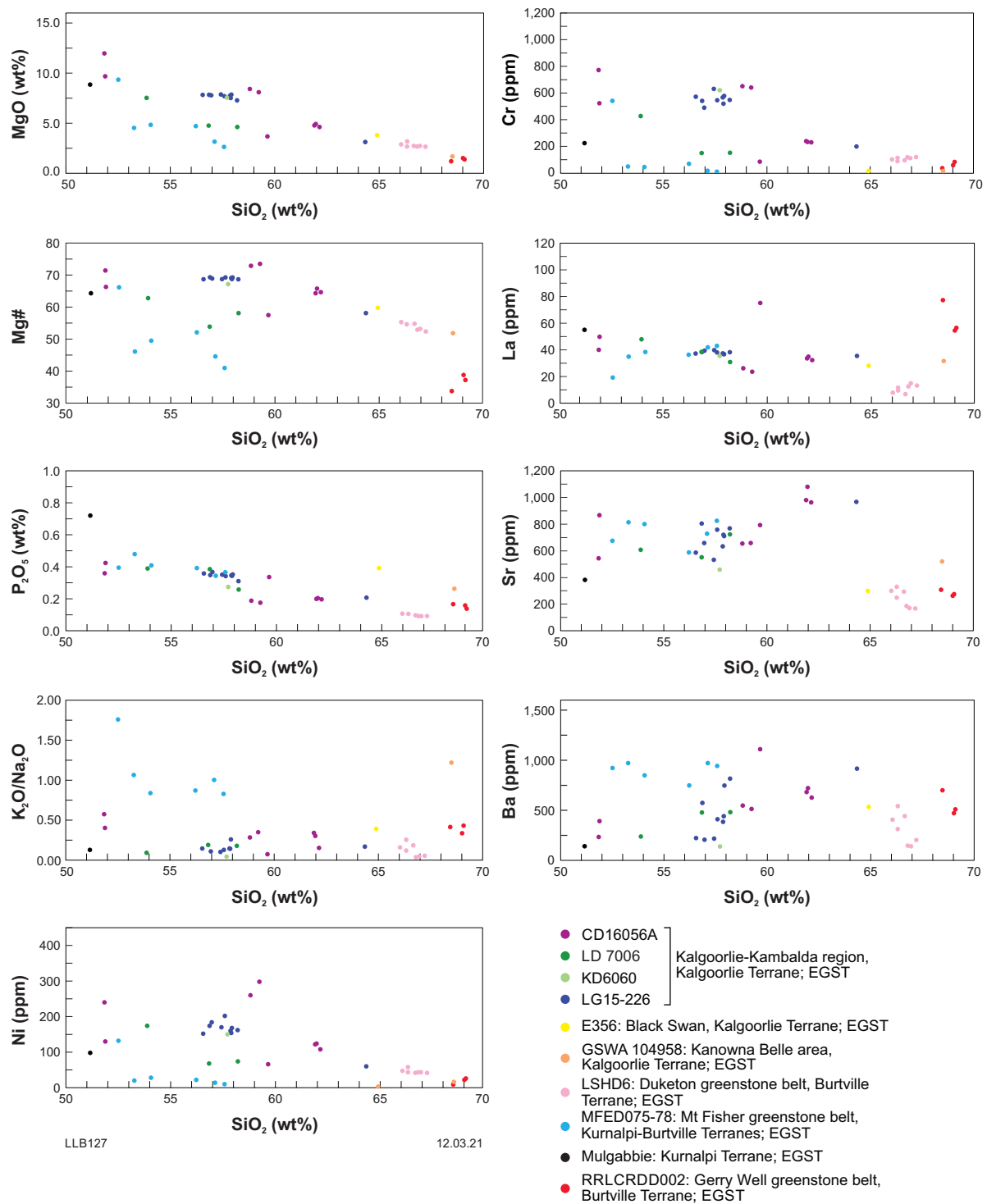


Figure 13. (above) Comparison of the chemistry between the sanukitoid-like units collected in this study from drillholes RRLCRDD002 and LSHD6, and other sanukitoids in the Eastern Goldfields Superterrane (most other data from Smithies et al., 2018). The data for four granodiorite samples from drillhole LSHD6 were obtained by the ALS laboratory using the MS81 method, except for Ni and Cr, which were obtained using the MS61L method

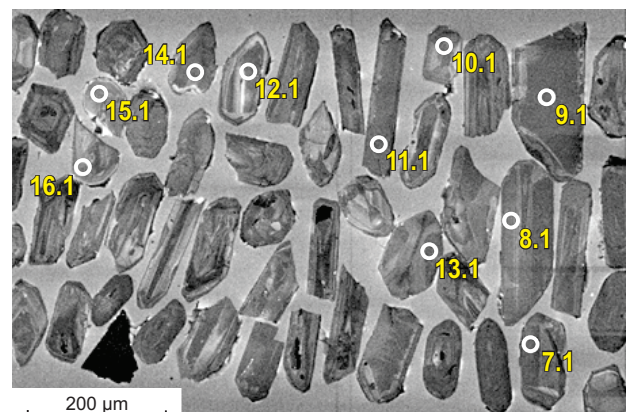


Figure 14. (right) Cathodoluminescence image of representative zircons from sample 235282. Numbered circles indicate the approximate locations of analysis sites from Lu et al. (2020)

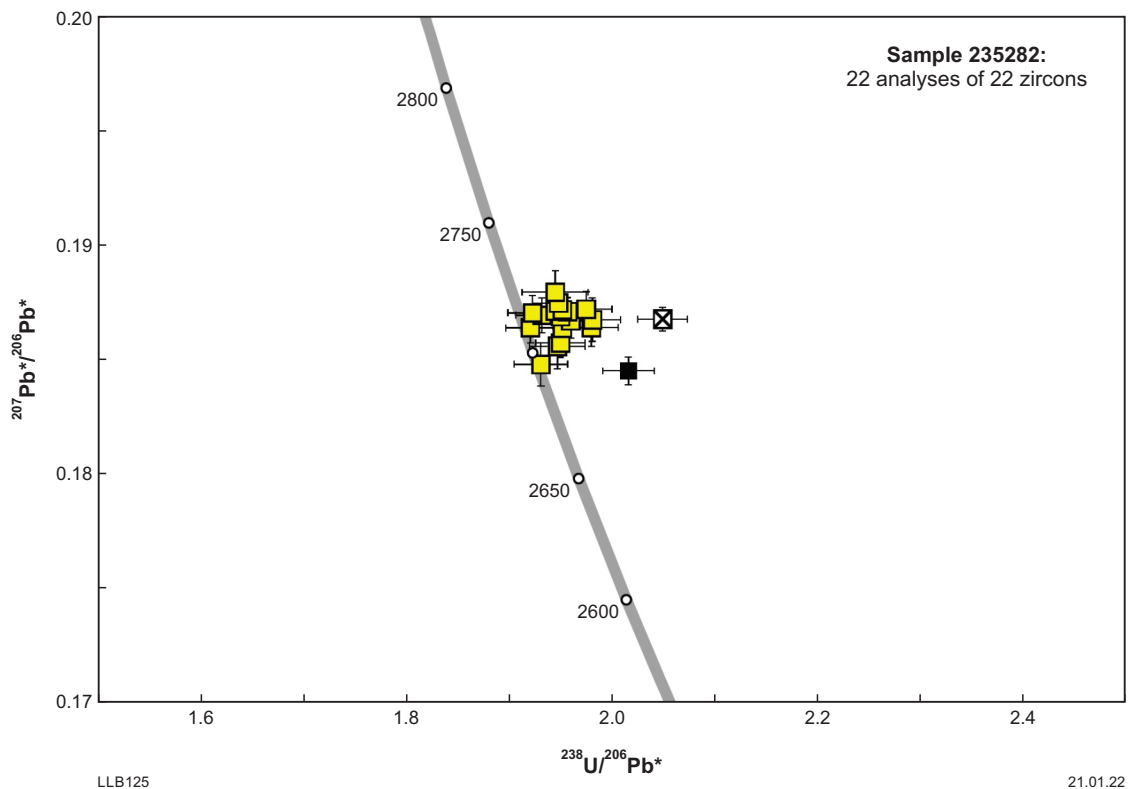


Figure 15. U–Pb analytical data for zircons from sample 235282. Yellow squares indicate Group I (magmatic zircons), black square indicates Group P (radiogenic-Pb loss), crossed square indicates Group D (discordance >5%). Two analyses from Group D are not shown (from Lu et al., 2020)

Significance of felsic magmatic events in the Collurabbie region

The sanukitoid-like unit in RRLCRDD002 (GSWA 235282) has an interpreted crystallization age of 2713 ± 3 Ma. It is interpreted from stratigraphic relationships in the drillcore to intrude sulfidic sediments, which are broadly contemporaneous with komatiites. This suggests that the komatiites were emplaced before 2713 ± 3 Ma, hence represent an event older than the highly mineralized 2.7 Ga komatiites in the Kalgoorlie Terrane. The komatiites in the Gerry Well greenstone belt could be related to the c. 2.8 Ga komatiites at Windarra (Barley et al., 2006) or the 2.84 – 2.94 Ga komatiites at Mt Fisher (Mole et al., 2016).

The age of the sanukitoid-like unit is also comparable with the interpreted magmatic ages of 2714 ± 5 Ma and 2719 ± 5 Ma, for two felsic igneous rock samples collected from drillcore LSHD6 in the Duketon greenstone belt (GSWA 153317; Nelson, 2004a; GSWA 153318; Nelson, 2004b). The newly determined geochemistry of these samples is also sanukitoid-like (Fig. 13), suggesting that there was a period of hydrous felsic magmatism throughout the Burtville Terrane that is significantly older than the 2.68 – 2.64 Ga lamprophyre-sanukitoid magmatic event recognized elsewhere in the EGST (Smithies et al., 2018).

It is notable that felsic rocks in other parts of the EGST have compositions and ages similar to the sanukitoid-like rocks in drillholes RRLCRDD002 (Gerry Well greenstone belt) and LSHD6 (Duketon greenstone belt). These include

a 2708 ± 7 Ma dacite (GSWA 104958, Fig. 13; Nelson, 1996) near Kanowna Belle, Kalgoorlie Terrane, which shows high P_2O_5/Nb chemistry (Smithies et al., 2018), and a 2712 ± 6 Ma volcanogenic conglomerate, which is intercalated with the komatiites at Black Swan in the Kalgoorlie Terrane (Sample number E356, Kositsin et al., 2008). The apparent rarity of felsic rocks with these characteristics in the Kalgoorlie Terrane compared to the well-documented 2.68 – 2.64 Ga sanukitoid event is not understood. However, their presence could indicate an earlier episode of widespread, hydrous felsic magmatism event with implications for gold mineralization (see below).

Mineralization potential of the Gerry Well greenstone belt

Nickel mineralization

No large komatiite-hosted nickel deposits have yet been found in the Gerry Well greenstone belt, although there is the relatively small Olympia deposit, with an inferred mineral resource of 573 000 tonnes grading 1.63% Ni, 1.19% Cu, 0.082% Co, 1.49 g/t Pd, and 0.85 g/t Pt (Rox Resources Limited, 2021). To establish whether the region is prospective for other larger deposits, we sought evidence for the occurrence of the six critical processes deemed necessary for their formation (applying a mineral systems analysis such as advocated by Wyborn et al., 1994):

1. generation of komatiitic magmas as a source for metals
2. lithospheric faulting to provide passage for transport of komatiitic magmas through the crust
3. assimilation of crustal sulfur by the magmas to induce saturation
4. sequestering of metals into sulfides
5. physical concentration of metal-rich sulfides
6. preservation of the nickel orebodies.

The presence of ultramafic rocks in the Collurabbie region clearly indicates that magmas of nominally appropriate composition were generated in the mantle, and that there were suitable pathways for transport of this magma through the crust.

The geochemistry of the ultramafic rocks in the Gerry Well greenstone belt suggests regional differences in mantle source compositions (Fig. 11). The $\text{Al}_2\text{O}_3/\text{TiO}_2$ ratios for those in the Far Northern Area (drillholes CXDD002-003) have an average of 15.2, which is similar to the 'type' in Al-depleted komatiites in the Barberton greenstone belt, South Africa (Nesbitt and Sun, 1976; Sun and Nesbitt, 1978; Nesbitt et al., 1979; Arndt et al., 2008), although the Collurabbie varieties are relatively high in TiO_2 (0.37 – 0.76 wt%). The highly altered ultramafic rocks from the Northern Ultramafic Portion (drillholes RRLCRDD005-006) have $\text{Al}_2\text{O}_3/\text{TiO}_2$ ratios ranging from 23.8 – 34.1 (averaging ~29), and fall below the 'chondritic mantle line', but they form a linear trend that most likely reflects primary igneous source compositions rather than alteration and is perhaps slightly Al-enriched (but not as enriched as komatiites in the Comondale greenstone belt, South Africa [Wilson, 2003]). Komatiites hosting the Fisher East nickel sulfide deposits in the Kurnalpi-Burtville Terrane to the west of Collurabbie (Fig. 1) have similar $\text{AlO}_2/\text{TiO}_2$ ratios, ranging from ~10–37 (average ~25; Burley and Barnes [2019]). Komatiite samples from the Southern Ultramafic Portion of the Gerry Well greenstone belt (drillholes RRLCRDD002–004) have $\text{Al}_2\text{O}_3/\text{TiO}_2$ ratios that fall mostly on or slightly above the 'chondritic mantle line', similar to most other komatiites in the EGST, for which there are data (Barnes, 2006). However, the $\text{Al}_2\text{O}_3/\text{TiO}_2$ ratio apparently has no bearing on the mineral potential of a komatiite, as nickel sulfide mineralization is known to occur in Al-depleted, Al-undepleted, and Al-enriched komatiites (Barnes and Fiorentini, 2012).

Ratios of TiO_2/Zr , Sm/La , Nb/Th , and Yb/Th are often used to determine whether komatiite melts have been contaminated with crustal material, hence by inference with the sulfur required to sequester metals into sulfides (Leshner, 1989). Only 10 out of the 64 komatiitic samples from the Gerry Well greenstone belt are considered to show some degree of crustal contamination (Figs 2, 9). Minimal contamination is also suggested by rare earth element patterns, which are relatively flat and lack light rare earth element enrichment in all samples except those from RRLCRDD007, CXDD002, and CXDD003 (Fig. 10; Barnes, 2006). These data and an absence of sulfide-bearing rocks in the drillcore indicate an apparent lack of sulfur sources in those parts of the crust sampled by diamond drilling or by the komatiites themselves.

Nickel sulfide mineralization in komatiitic rocks is preferentially concentrated in olivine cumulate-rich channels

that were subject to high magma flux (Barnes et al., 2004). Komatiites in the Collurabbie region are typically so altered that such indicative primary magmatic textures and mineralogy are obscured. However, different flow facies are chemically different, and can be discriminated using ratios of elements such as Ni, Ti, and Cr that are typically immobile during hydrothermal alteration (Le Vaillant et al., 2016). Apart from a few outliers, the compositions of the majority of the Collurabbie komatiites plot in zones characteristic of spinifex flow-top and orthocumulate (channel) facies. Many samples fall in the overlap between these facies zones, but a significant proportion of those from drillholes RRLCRDD003, RRLCRDD004, and RRLCRDD006 plot in the chromite-rich cumulate zone (Fig. 7). Ultramafic rock units are also particularly thick in these drillholes, and the presence of channel facies komatiites is therefore, strongly supported at these locations. This notwithstanding, the ultramafic geochemistry and sporadically preserved primary magmatic textures indicate that many of the komatiitic rocks in the area are probably spinifex-textured or flow-top units, possibly from 'flanking' environments. The cumulate (channel) facies rocks are also generally relatively Ni-poor, and all samples lie on the barren-komatiite trend (Figure 8).

The overall impression is that the Collurabbie region has some features favourable for Ni sulfide mineralization, but the ultramafic rocks did not assimilate significant crustal sulfur; hence, did not achieve sulfur saturation and precipitate sulfides. However, the existence of the Olympia deposit indicates that sulfur saturation occurred at least locally in ultramafic rocks, and that further work is required to understand this discrepancy and the true prospectivity of the Collurabbie region for komatiite-hosted nickel.

Gold mineralization

There is a widely acknowledged spatial and temporal correlation between gold mineralization, lamprophyres and sanukitoids (e.g. Rock and Groves, 1988b; Rock and Groves, 1988a; Rock et al., 1989; Witt et al., 2013; Witt et al., 2015). The potential for lamprophyres or sanukitoids to be sources for gold is unknown, but transport and emplacement of their primary magmas are believed to have been controlled by trans-lithospheric structures that were also important conduits for large volumes of hydrothermal fluids that transport gold scavenged from the mantle or crust (Smithies et al., 2018). Smithies et al. (2018) note that 2.66 – 2.64 Ga gold mineralization in the Kalgoorlie-Kurnalpi terrane is commonly hosted by the Black Flag Group, which they believe is largely the extrusive or subvolcanic equivalent of a 2.68 – 2.66 Ga lamprophyre-sanukitoid magmatic event. They imply that these magmas transported gold from their metasomatized mantle source into the crust, where it could be subsequently remobilized by later hydrothermal events.

If sanukitoids are related to gold mineralization, then any newly recognized sanukitoid occurrences may indicate the presence of lithospheric structures that may have also focused on different types of metalliferous mineralization. The 2713 ± 3 Ma sanukitoid-like rock in the Collurabbie region could also possibly signal the occurrence of a corresponding, unrecognized gold mineralizing event older than that known in the EGST. Recently discovered gold mineralization in the Collurabbie region (e.g. the Naxos prospect; Rox Resources Limited, 2021) may be part of such an older event.

Conclusion

New mineralogical, geochemical, and geochronological data from eight diamond drillcores from the western part of the Gerry Well greenstone belt (Collurabbie region) in the Burtville Terrane, northeastern Yilgarn Craton have improved our understanding of its lithostratigraphy, age, geochemical characteristics and prospectivity for nickel and gold mineral systems.

Mantle-derived ultramafic rocks in the region locally show many compositional, textural and mineralogical features that are considered necessary indicators of economic Ni sulfide prospectivity, except that there is little evidence for assimilation of the crustal sulfur that is presumed to be required for the scavenging of nickel and other metals from the ultramafic magmas into sulfides. The absence of this one critical component; therefore, suggests that the prospectivity of the Gerry Well greenstone belt for major nickel sulfide deposits is comparatively low. However, only a small portion of the greenstone belt has been examined in any detail, and the recent discovery of the sub-economic Olympia Ni–Cu–Co–platinoid deposit indicates that further work is required to understand the Ni sulfide mineralizing processes, and the metallogenic potential of the Collurabbie region.

A sanukitoid-like felsic igneous rock with an age of 2713 ± 3 Ma is interpreted to be younger than the komatiites in the Gerry Well greenstone belt, indicating that these komatiites are older than the c. 2.7 Ga varieties that predominate in the Kalgoorlie Terrane and are hosts to significant Ni sulfide deposits. Sanukitoid-like rocks with ages of 2714 ± 5 Ma and 2719 ± 5 Ma are also now recognized in the Duketon greenstone belt, suggesting that sanukitoid magmatism may have been widespread in the Burtville Terrane, and be older than the well-documented (2.68 – 2.66 Ga) sanukitoid magmatism in the Kalgoorlie Terrane. Sanukitoids are believed to be significant empirical indicators of gold prospectivity because of their apparent close spatial and temporal association with gold mineralization. The possible occurrence of an older sanukitoid magmatic event in the Burtville Terrane might, therefore, indicate prospectivity for an older gold mineralizing event in the EGST.

Acknowledgements

This study was undertaken as part of a collaborative research program on magmatic nickel sulfide mineralization by GSWA and the Xi'an Centre of the China Geological Survey. The authors thank Regis Resources for providing access to the drillcores, datasets, and logistical support that contributed to this study.

References

- Allibone, AH, Windh, J, Etheridge, MA, Burton, D, Anderson, G, Edwards, PE, Miller, A, Graves, C, Fanning, CM and Wysoczanski, R 1998, Timing relationships and structural controls on the location of Au–Cu mineralization at the Boddington gold mine, Western Australia: *Economic Geology*, v. 93, p. 245–270.
- Arndt, NT, Leshner, CM and Barnes, SJ 2008, *Komatiite*: Cambridge University Press, Cambridge, UK, 467p.
- Baggot, M 2006, A refined model for the magmatic, tectonometamorphic and hydrothermal evolution of the Leonora district, Eastern Goldfields Province, Yilgarn Craton, Western Australia: Ph.D. thesis, University of Western Australia.
- Barley, ME, Brown, SJA and Krapež, B 2006, Felsic volcanism in the eastern Yilgarn Craton, Western Australia: Evolution of a late Archean convergent margin: *Geochimica et Cosmochimica Acta*, v. 70, A35.
- Barley, ME, Stuart, JA, Krapež, B and Kositsin, N 2008, Physical volcanology and geochemistry of a late Archean volcanic arc: Kurnalpi and Gindalbie terranes, eastern goldfields Superterrane, Western Australia: *Precambrian Research*, v. 161, p. 53–76.
- Barnes, SJ (editor) 2006, Nickel deposits of the Yilgarn Craton: Geology, geochemistry, and geophysics applied to exploration: Society of Economic Geologists, Special Publication 13, 210p.
- Barnes, SJ and Fiorentini, ML 2012, Komatiite magmas and sulfide nickel deposits: A comparison of variably endowed Archean Terranes: *Economic Geology*, v. 107, p. 755–780.
- Barnes, SJ, Hill, RET, Perring, CS and Dowling, SE 2004, Lithogeochemical exploration of komatiite-associated Ni-sulfide deposits: Strategies and limitations: *Mineralogy and Petrology*, v. 82, p. 259–293.
- Barnes, SJ, Van Kranendonk, MJ and Sonntag, I 2012, Geochemistry and tectonic setting of basalts from the Eastern Goldfields Superterrane, Yilgarn Craton: *Australian Journal of Earth Sciences*, v. 59, no. 5, p. 707–735.
- Brand, NW 1999, Element ratios in nickel sulfide exploration: vectoring towards ore environments: *Journal of Geochemical Exploration*, v. 67, no. 1–3, p. 145–165.
- Brown, SJA, Barley, ME, Krapež, B and Cas, RAF 2002, The late Archean Melita Complex, eastern goldfields, Western Australia: Shallow submarine bimodal volcanism in a rifted arc environment: *Journal of Volcanological and Geothermal Research*, v. 115, p. 303–327.
- Burley, LL and Barnes, SJ 2019, Komatiite characteristics of the Fisher East nickel sulfide prospects: implications for nickel prospectivity in the northeastern Kurnalpi Terrane: Geological Survey of Western Australia, Report 198, 27p.
- Campbell, IH and Hill, RI 1988, A two-stage model for the formation of the granite-greenstone terrane of the Kalgoorlie-Norseman area, Western Australia: *Earth and Planetary Science Letters*, v. 90, p. 11–25.
- Cassidy, KF, Champion, DC, Krapež, B, Barley, ME, Brown, SJ, Blewett, RS, Groenewald, PB and Tyler, IM 2006, A revised geological framework for the Yilgarn Craton, Western Australia: Geological Survey of Western Australia, Record 2006/8, 8p.
- Cassidy, KF, Champion, DC, McNaughton, N, Fletcher, IR, Whitaker, AJ, Bastrakova, IV and Budd, A 2002, The characterisation and metallogenic significance of Archaean granitoids of the Yilgarn Craton, Western Australia: Minerals and Energy Research Institute of Western Australia, MERIWA Project no. M281/AMIRA Project no. 482 (Report No. 222).
- Champion, DC and Sheraton, JW 1997, Geochemistry and Nd isotope systematics of Archaean granites of the Eastern Goldfields, Yilgarn Craton, Australia: implications for crustal growth processes: *Precambrian Research*, v. 83, no. 1–3, p. 109–132, doi:10.1016/S0301-9268(97)00007-7.

- Champion, DC and Stewart, AJ 1996, Uraey, WA sheet 3343 (preliminary edition): Australian Geological Survey Organisation, 1:100 000 Geological Series.
- Chen, SF, Riganti, A, Wyche, S, Greenfield, JE and Nelson DR 2003, Lithostratigraphy and tectonic evolution of contrasting greenstone successions in the central Yilgarn craton, Western Australia: *Precambrian Research*, v. 127, p. 249–266.
- Cudahy, TJ, Jones, M, Thomas, M, Laukamp, C, Caccetta, M, Hewson, RD, Rodger, AR and Verrall, M 2008, Next generation mineral mapping: Queensland airborne HyMap and satellite ASTER surveys 2006–2008: Commonwealth Scientific and Industrial Research Organisation, Open File Report P2007/364, 120p.
- Czarnota, K, Blewett, RS and Goscombe, B 2008, Structural and metamorphic controls on gold through time and space in the Central Eastern Goldfields Superterrane – a field guide: Geological Survey of Western Australia, Record 2008/9, 66p.
- Czarnota, K, Champion, DC, Cassidy, KF, Goscombe, B, Blewett, R, Henson, PA and Groenewald, PB 2010, Geodynamics of the eastern Yilgarn Craton: *Precambrian Research*, v. 183, p. 175–202.
- Dunphy, JM, Fletcher, IR, Cassidy, KF and Champion, DC 2003, Compilation of SHRIMP U-Pb geochronological data, Yilgarn craton, Western Australia, 2001–02: Geoscience Australia, Record 2003/15, 147p.
- Dykman, SE 2008, Combined annual report on exploration for the period 30/04/2007 to 29/04/2008: Collurabie Project C32/1999, E38/241, E38/423, E38/464, E38/465, E38/510, E38/511, E38/1021, E38/1104, E38/1135, E38/1182, E38/1307, E38/1308, E38/1314, E38/1412, E38/1413, E38/1436, E38/1595, E38/1596, E38/1597, M38/903, M38/904, M38/925: Regis Resources Ltd: Geological Survey of Western Australia, Statutory mineral exploration report A78701, 19p.
- Hancock, EA, Duuring, P, Guiliamse, JN, Burley, L and Wawryk, M 2020, Compilation of HyLogger records, 2020: Geological Survey of Western Australia non-series data package.
- Hancock, EA, Green, AA, Huntington, JF, Schodlok, MC and Whitbourn, LB 2013, HyLogger-3: implications of adding thermal-infrared sensing: Geological Survey of Western Australia, Record 2013/3, 24p.
- Hancock, EA and Huntington, JF 2010, The GSWA HyLogger: Rapid spectral analysis and its application in detecting mineralization, in GSWA extended abstracts: promoting the prospectivity of Western Australia: Geological Survey of Western Australia, Record 2010/2, p. 10–13.
- Huntington, JF, Mason, P and Berman, M 1997, Geological evaluation of The Spectral Assistant (TSA) for mineralogical interpretation: Commonwealth Scientific and Industrial Research Organisation, Exploration and Mining Report 417R, 86p.
- Ivanic, TJ, Wingate, MTD, Kirkland, CL, van Kranendonk, M and Wyche S 2010, Age and significance of voluminous mafic-ultramafic magmatic events in the Murchison domain, Yilgarn craton, Western Australia: *Australian Journal of Earth Science*, v. 57, p. 597–614.
- Ivanic, TJ, van Kranendonk, MJ, Kirkland, CL, Wyche, S, Wingate, MTD and Belousova, EA 2012, Zircon Lu-Hf isotopes and granite geochemistry of the Murchison domain of the Yilgarn craton: Evidence for reworking of Eoarchean crust during Meso-Neoproterozoic plume-driven magmatism: *Lithos*, v. 148, p. 112–127.
- Jones, JA 2006, Collurabie, WA Sheet 3344: Geological Survey of Western Australia, 1:100 000 Geological Series.
- Kinny, PD, Williams, IS, Froude, DO, Ireland, TR and Compston, W 1988, Early Archean zircon ages from orthogneisses and anorthosites at Mount Narryer: *Precambrian Research*, v. 38, p. 325–341.
- Kositcin, N, Brown, SJA, Barley, ME, Krapež, B, Cassidy, KF and Champion, DC 2008, SHRIMP U-Pb zircon age constraints on the Late Archean tectonostratigraphic architecture of the Eastern Goldfields Superterrane, Yilgarn Craton, Western Australia: *Precambrian Research*, v. 161, p. 5–33.
- Krapež, B and Pickard, A 2010, Detrital-zircon age spectra for late Archean synorogenic basins of the eastern goldfield Superterrane, Western Australia: *Precambrian Research*, v. 178, p. 91–118.
- Le Vaillant, M, Fiorentini, ML and Barnes, SJ 2016, Review of lithochemical exploration tools for komatiite-hosted Ni–Cu–(PGE) deposits: *Journal of Geochemical Exploration*, v. 168, p. 1–19, doi:10.1016/j.gexplo.2016.05.010.
- Leshner, CM 1989, Komatiite-associated nickel sulfide deposits, in *Ore deposition associated with magmas edited by* JA Whitney, AJ Naldrett and JM Robertson, *Reviews in Economic Geology*, p. 44–101, doi:10.5382/Rev.04.05.
- Lu, Y, Wingate, MTD and Grech, LL 2020, 235282: altered tonalite, Jerrys Bore; *Geochronology Record* 1687: Geological Survey of Western Australia, 4p.
- Martin, DMCB, Hocking, RM, Riganti, A and Tyler, IM 2016a, 1:10 000 000 tectonic units of Western Australia: Geological Survey of Western Australia, digital data layer, <www.dmirs.wa.gov.au/geoview>.
- Martin, DMCB, Johnson, SP and Riganti, A 2016b, 1:500 000 State interpreted bedrock geology of Western Australia, 2016: Geological Survey of Western Australia, digital data layer, <www.dmirs.wa.gov.au/geoview>.
- Martin, H, Smithies, RH, Rapp, R, Moyen, J-F and Champion, DC 2005, An overview of adakite, tonalite–trondhjemite–granodiorite (TTG), and sanukitoid: relationships and some implications for crustal evolution: *Lithos*, v. 79, p. 1–24, doi:10.1016/j.lithos.2004.04.048.
- McDonough, WF and Sun, S-S 1995, The composition of the Earth: *Chemical Geology*, v. 120, p. 223–253.
- Mole, DR, Fiorentini, ML, Thebaud, N, McCuaig, TC, Cassidy, KF, Kirkland, CL, Wingate, MTD, Romano, SS, Doublier, MD and Belousova EA 2012, Spatio-temporal constraints on lithospheric development in the southwest-central Yilgarn craton: *Australian Journal of Earth Science*, v. 59, p. 625–656.
- Mole, DR, Fiorentini, ML, Cassidy, KF, Kirkland, CL, Thebaud, N, McCuaig, TC, Doublier, MP, Duuring, P, Romano, SS, Maas, R, Belousova, EA, Barnes SJ and Miller, J 2013, Crustal evolution, intra-cratonic architecture and the metallogeny of an Archean craton: *Geological Society of London Special Publication*, v. 393, p. 23–80, doi.org/10.1144/SP393.8.
- Mole, DR, Burley, L and Barnes, SJ 2016, A new komatiite-hosted Ni–Cu–PGE event in the Eastern Goldfields Superterrane, in *13th International Ni–Cu–PGE symposium, Fremantle, Australia: Abstracts edited by* B Godel, S Barnes, I Gonzalez-Alvarez, M Fiorentini and M Le Vaillant: Geological Survey of Western Australia, Record 2016/13, p. 57.
- Morris, PA and Kirkland, CL 2014, Melting of a subduction-modified mantle source: A case study from the Marda Volcanic Complex, central Yilgarn craton, Western Australia: *Lithos*, v. 190, p. 403–419.
- Nelson, DR 1996, 104958: dacite, Ballarat – Last Chance; *Geochronology Record* 20: Geological Survey of Western Australia, 6p.
- Nelson, DR 1997, Evolution of the Archean granite-greenstone terranes of the Eastern Goldfields, Western Australia: SHRIMP U-Pb zircon constraints: *Precambrian Research*, v. 83, no. 1–3, p. 57–81.
- Nelson, DR 2004a, 153317: dacite, Duketon Battery; *Geochronology Record* 72: Geological Survey of Western Australia, 4p.
- Nelson, DR 2004b, 153318: dacite, Duketon Battery; *Geochronology Record* 64: Geological Survey of Western Australia, 4p.
- Nesbitt, RW and Sun, SS 1976, Geochemistry of Archean spinifex textures peridotites and magnesian and low magnesian tholeiites: *Earth and Planetary Science Letters*, v. 31, p. 433–453.
- Nesbitt, RW, Sun, S-S and Purvis, AC 1979, Komatiites: *Geochemistry and genesis: Canadian Mineralogist*, v. 17, p. 165–186.
- Pawley, MJ, Wingate, MTD, Kirkland, CL, Wyche, S, Hall, CE, Romano, SS and Doublier, MP 2012, Adding pieces to the puzzle: Episodic crustal growth and a new terrane in the northeast Yilgarn craton, Western Australia: *Australian Journal of Earth Science*, v. 59, p. 603–623.
- Perring, CS and Rock, NMS 1991, Relationships between acidic (dacitic) and primitive (lamprophyric) magmas in late Archean composite dykes: *Precambrian Research*, v. 52, p. 245–273.
- Pidgeon, RT and Wilde, SA 1990, The distribution of 3.0 Ga and 2.7 Ga volcanic episodes in the Yilgarn craton of Western Australia: *Precambrian Research*, v. 48, p. 309–325.
- Rasmussen, B, Fletcher, IR, Muhling, J, Gregory, CJ and Wilde, SA 2011, Metamorphic replacement of mineral inclusions in detrital zircons from Jack Hills, Australia: Implications for the Hadean Earth: *Geology*, v. 39, p. 1143–1146.
- Rock, N and Groves, DI 1988a, Do lamprophyres carry gold as well as diamonds? *Nature*, v. 332, p. 253–255.

- Rock, NMS and Groves, DI 1988b, Can lamprophyres resolve the genetic controversy over mesothermal gold deposits? *Geology*, v. 16, p. 538–541.
- Rock, NMS, Groves, DI, Perring, CS and Golding, SD 1989, Gold, lamprophyres, and porphyries: What does their association mean? *in* The Geology of Gold Deposits: the Perspective in 1988 *edited by* RR Keays, WRH Ramsay and DI Groves: Economic Geology Monograph 6, p. 609–625.
- Romano, SS, Doublier, MD, Mole, DR, Thebaud, N, Wingate, MTD and Kirkland, C 2010, Age constraints in the southern part of the southern cross domain of the Yilgarn craton: Geological Survey of Western Australia, Record 2010/8, p. 206–208.
- Rox Resources Limited 2021, Quarterly report for the period ending 31 December 2020; Report to Australian Securities Exchange, released 29-01-2021.
- Schodlok, MC, Whitbourn, L, Huntington, J, Mason, P, Green, A, Berman, M, Coward, D, Connor, P, Wright, W, Jolivet, M and Martinez, R 2016, HyLogger-3, a visible to shortwave and thermal infrared reflectance spectrometer system for drillcore logging: functional description: *Australian Journal of Earth Sciences*, v. 63, no. 8, p. 929–940, doi:10.1080/08120099.2016.1231133.
- Shirey, SB and Hanson, GN 1984, Mantle-derived Archaean monzoniorites and trachyandesites: *Nature*, v. 310, p. 222–224.
- Smithies, RH and Champion, DC 2000, The Archaean high-Mg diorite suite: links to tonalite-trondhjemite-granodiorite magmatism and implication for early Archaean crustal growth: *Journal of Petrology*, v. 41, no. 12, p. 1653–1671.
- Smithies, RH, Lu, Y, Kirkland, CL, Cassidy, KF, Champion, DC, Sapkota, J, de Paoli, M and Burley, L 2018, A new look at lamprophyres and sanukitoids, and their relationship to the Black Flag Group and gold prospectivity: Geological Survey of Western Australia, Record 2018/15, 23p.
- Smithies, RH, Morris, PA, Wyche, S, de Paoli, M and Sapkota, J 2017, Towards a geochemical barcode for Eastern Goldfields Superterrane greenstone stratigraphy - preliminary data from the Kambalda-Kalgoorlie area: Geological Survey of Western Australia, Record 2017/7, 26p.
- Squire, RJ, Allen, CM, Cas, RAF, Campbell, IH, Blewett, RS and Nemchin, AA 2010, Two cycles of pyroclastic volcanism and sedimentation related to episodic granite emplacement during the late Archaean, eastern Yilgarn craton, Western Australia: *Precambrian Research*, v. 183, p. 251–274.
- Stein, H, Markey, RJ, Morgan, JW, Selby, D, Creaser, RA, McCuaig, TC and Behn M 2001, Re-Os dating of Boddington molybdenite, SW Yilgarn: Two gold mineralization events: AGSO-Geoscience Australia, Record 2001/37, p. 469–471.
- Stern, RA, Hanson, GN and Shirey, SB 1989, Petrogenesis of mantle-derived, LILE-enriched Archaean monzoniorites and trachyandesites (sanukitoids) in southwestern Superior Province: *Canadian Journal of Earth Sciences*, v. 26, p. 1688–1712.
- Sun, SS and Nesbitt, RW 1978, Petrogenesis of Archaean ultrabasic and basic volcanics: evidence from rare earth elements: *Contributions to Mineralogy and Petrology*, v. 65, p. 301–325.
- Sun, S-S and McDonough, WF 1989, Chemical and isotopic systematics of oceanic basalts: implications for mantle composition and processes, *in* *Magmatism in the Ocean Basins* *edited by* AD Saunders and MJ Norry: The Geological Society of London, Special Publication 42, p. 313–345.
- Swager, CP 1997, Tectono-stratigraphy of late Archaean greenstone terranes in the southern Eastern Goldfields, Western Australia: *Precambrian Research*, v. 83, p. 11–42.
- Swager, CP, Witt, WK, Griffin, TJ, Ahmat, AL, Hunter, WM, McGoldrick, PJ and Wyche, S 1992, Late Archaean granite-greenstones of the Kalgoorlie Terrane, Yilgarn Craton, Western Australia, *in* The Archaean: Terrains, processes and metallogeny: Proceedings for the Third International Archaean Symposium, *edited by* JE Glover and SE Ho: Geology Department and University Extension, The University of Western Australia, Perth, Western Australia, Publication 22, 17–21 September 1990 p. 107–122.
- Thebaud, N and Miller J 2009, U-Pb age constraint on the siliciclastic sediments from the upper supracrustal cover in the southern cross greenstone belt, Youanmi terrane, Western Australia, *in* Smart science for exploration and mining *edited by* PJ Williams: Proceedings of the Tenth Biannual SGA Meeting, Townsville, Queensland, Abstract Volume, p. 960–962.
- Thern, ER and Nelson, DR 2012, Detrital zircon age structure within ca 3 Ga metasedimentary rocks, Yilgarn craton: Elucidation of Hadean source terranes by principal component analysis: *Precambrian Research*, v. 214, p. 28–43.
- Van Kranendonk, MJ and Ivanic, TJ 2009, A new lithostratigraphic scheme for the northeastern Murchison domain, Yilgarn craton: Geological Survey of Western Australia Annual Review 2007-08, p. 34–53.
- Wilde, SA and Pidgeon, RT 1986, Geology and geochronology of the Saddleback greenstone belt in the Archaean Yilgarn block, southwestern Australia: *Australian Journal of Earth Science*, v. 33, p. 491–450.
- Wilde, SA, Middleton, MF and Evans, BJ 1996, Tectonic accretion in the southwestern Yilgarn craton: Evidence from a deep seismic crustal profile: *Precambrian Research*, v. 78, p. 179–196.
- Wilson, AH 2003, A new class of silica enriched, highly depleted komatiites in the southern Kapaal Craton, South Africa: *Precambrian Research*, v. 127, p. 125–141.
- Witt, WK 1998, Geology and mineral resources of the Ravensthorpe and Cocanarup 1:100 000 sheets: Geological Survey of Western Australia, Report 54, 152p.
- Witt, WK, Stein, H, Cassidy, KF, Black, L, Champion, DC and Fletcher, IR 2001, A >2.75Ga basement enclave at Leonora: A domain of uplift and >2.75 Ga gold within the 2.71-2.66 Ga Eastern Goldfields Province, *in* AGU Chapman Conference, Dunsborough, Western Australia, abstracts volume.
- Witt, WK, Cassidy, KF, Lu, YJ and Hagemann, SG 2020, The tectonic setting and evolution of the 2.7 Ga Kalgoorlie-Kurnalpi Rift, a world-class Archaean gold province: *Mineralium Deposita*, v. 55, p. 601–631.
- Witt, WK, Ford, A and Hanrahan, B 2015, District-scale targeting for gold in the Yilgarn Craton: Part 2 of the Yilgarn Gold Exploration Targeting Atlas: Geological Survey of Western Australia, Report 132, 276p.
- Witt, WK, Ford, A, Hanrahan, B and Mamuse, A 2013, Regional-scale targeting for gold in the Yilgarn Craton: Part 1 of the Yilgarn Gold Exploration Targeting Atlas: Geological Survey of Western Australia, Report 125, 130p.
- Wyborn, LAI, Heinrich, CA and Jaques, AL 1994, Australian Proterozoic mineral systems: Essential ingredients and mappable criteria *edited by* P Hallenstein: 1994 AusIMM Annual Conference, Darwin, Northern Territory, 1994/08/05: Australian Institute of Mining and Metallurgy, Australian mining looks north – the challenges and choices, p. 109–115.
- Wyche, S, Nelson, DR and Riganti, A 2004, 4350-3130 Ma detrital zircons in the southern cross granite – Greenstone terrane, Western Australia: Implications for the early evolution of the Yilgarn craton: *Australian Journal of Earth Science*, v. 51, p. 31–45.

RECORD 2022/2

GEOLOGY AND MINERALIZATION POTENTIAL OF THE GERRY WELL GREENSTONE BELT (COLLURABBIE REGION), NORTHEASTERN YILGARN CRATON

LL Grech, Y Lu, Y Wang, Y Gao, B Qian, M You and TJ Beardsmore

Access GSWA products



All products

All GSWA products are free to download as PDFs from the DMIRS eBookshop
<www.dmirs.wa.gov.au/ebookshop>. View other geoscience
information on our website <www.dmirs.wa.gov.au/gswa>.



Hard copies

Limited products are available to purchase as hard copies from the
First Floor counter at Mineral House or via the DMIRS eBookshop
<www.dmirs.wa.gov.au/ebookshop>.



Fieldnotes

Fieldnotes is a free digital-only quarterly newsletter which provides
regular updates to the State's exploration industry and geoscientists
about GSWA's latest programs, products and services.
Access by subscribing to the GSWA eNewsletter
<www.dmirs.wa.gov.au/gswaenewsletter> or downloading the free
PDF from the DMIRS eBookshop <www.dmirs.wa.gov.au/ebookshop>.



GSWA eNewsletter

The GSWA eNewsletter is an online newsletter that contains
information on workshops, field trips, training and other events.
To keep informed, please subscribe
<www.dmirs.wa.gov.au/gswaenewsletter>.



Further details of geoscience products are available from:

First Floor Counter
Department of Mines, Industry Regulation and Safety
100 Plain Street
EAST PERTH WESTERN AUSTRALIA 6004
Phone: +61 8 9222 3459 Email: publications@dmirs.wa.gov.au
www.dmirs.wa.gov.au/GSWApublications